Fall 1994

# An adaptive asynchronous CDMA receiver and its convergence analysis

Lizhi Zhong
*New Jersey Institute of Technology*

# Copyright Warning & Restrictions

The copyright law of the United States (Title 17, United States Code) governs the making of photocopies or other reproductions of copyrighted material.

Under certain conditions specified in the law, libraries and archives are authorized to furnish a photocopy or other reproduction. One of these specified conditions is that the photocopy or reproduction is not to be "used for any purpose other than private study, scholarship, or research." If a, user makes a request for, or later uses, a photocopy or reproduction for purposes in excess of "fair use" that user may be liable for copyright infringement,

This institution reserves the right to refuse to accept a copying order if, in its judgment, fulfillment of the order would involve violation of copyright law.

Please Note: The author retains the copyright while the New Jersey Institute of Technology reserves the right to distribute this thesis or dissertation

Printing note: If you do not wish to print this page, then select "Pages from: first page # to: last page #" on the print dialog screen

# ABSTRACT

## AN ADAPTIVE ASYNCHRONOUS CDMA RECEIVER AND ITS CONVERGENCE ANALYSIS

by
**Lizhi Zhong**

An adaptive CDMA receiver scheme assuming perfect synchronization has been generalized in this thesis to the asynchronous channel, a much more practical assumption of the real system. Similar formulas are derived and as its synchronous version, it is still near-far resistant and requires no knowldge of received signal amplitudes and training sequences. Thus, sophisticated high-precision power control and user power estimation are not necessary and the receiver is particularly useful in mobile communications since it can adjust itself adaptively to changes in the power of the users. The convergence and transient behavior of the receiver are also investigated and found to have similar results to its synchronous counterpart.

A new way to analyze the error performance of the decorrelator is also proposed and the error probability of the one-shot decorrelator is formulated for the general case in an alternative way using the new idea, which is much simpler. Furthermore, the singularity problem associated with the one-shot decorrelator is addressed and its effect on the performance of the receiver is discussed.

# AN ADAPTIVE ASYNCHRONOUS CDMA RECEIVER AND ITS CONVERGENCE ANALYSIS

by
Lizhi Zhong



A Thesis
Submitted to the Faculty of
New Jersey Institute of Technology
in Partial Fulfillment of the Requirements for the Degree of
Master of Science in Electrical Engineering

Department of Electrical and Computer Engineering

January 1995

## APPROVAL PAGE

# AN ADAPTIVE ASYNCHRONOUS CDMA RECEIVER AND ITS CONVERGENCE ANALYSIS

**Lizhi Zhong**

---

Dr. Zoran Siveski, Thesis Advisor — Date
Assistant Professor of Electrical and Computer Engineering
New Jersey Institute of Technology

---

Dr. Nirwan Ansari, Committee Member — Date
Associate Professor of Electrical and Computer Engineering
New Jersey Institute of Technology

---

Dr. Yeheskel Bar-Ness, Committee Member — Date
Distinguished Professor of Electrical and Computer Engineering
New Jersey Institute of Technology

## BIOGRAPHICAL SKETCH

**Author:** Lizhi Zhong

**Degree:** Master of Science in Electrical Engineering

**Date:** January 1995

### Undergraduate and Graduate Education:

- Master of Science in Electrical Engineering,
  New Jersey Institute of Technology,
  Newark, New Jersey, 1995
- Bachelor of Science in Electrical Engineering,
  Tsinghua University,
  Beijing, P.R.China, 1993

**Major:** Electrical Engineering

### Presentations and Publications:

Z. Siveski, L. Zhong and Y. Bar-Ness, "Adaptive Multiuser CDMA Detector for Asynchronous AWGN Channels," *Presented in the 5th IEEE International Symposium on Personal, Indoor and Mobile Radio Communications*, The Hague, The Netherlands, Sept. 1994.

This thesis is dedicated to Mom, Dad
and my dear sister, Dena.

## ACKNOWLEDGMENT

I would like to acknowledge the help of several individuals in the preparation of this thesis. First and foremost, I must thank Dr. Zoran Siveski for his useful suggetions and kind assistance throughout the writing of the thesis. I would also like to thank Dr. Nirwan Ansari, who gave me valuable advice, and Prof. Yeheskel Bar-Ness, who took a special interest and provided timely support.

I have benefited greatly from David Chen, who supplied me with the programs for the synchronous case of the detector and who gave me indispensable help in the programming details. I would particularly like to express my appreciation to Frank Viehofer, whose partnership I cherish.

I feel extremely fortunate to have worked with Lisa Fitton, Susan Wu, Xinyu Huang, Sandra Liu, Sarah Zhu, Gangsheng Wang, Murali Arulambalam, Amit Shah and all the friends in the Center for Communications and Signal Processing.

Most of all, I would like to thank my parents and my sister, for all their love and support.

## TABLE OF CONTENTS

## LIST OF FIGURES

# CHAPTER 1

# INTRODUCTION

Code division multiple access (CDMA) is the future of digital communications. With increased capacity, improved quality and greater coverage, it is the long-term answer to the cellular industry's most pressing issues. Actually, the Interim Standard 95 (IS-95) of CDMA was adopted by the Telecommunications Industry Association (TIA) in 1993.

While it becomes more and more interesting to the industry, the research on CDMA in academia has been ongoing for more than ten years. The conventional single-user detector was found to be unfit for multiuser detection since it ignores the presence of multiaccess interference and therefore suffers severe performance degradation in the presence of strong interference, which is called the "near-far" problem. To cope with that, sophisticated high-precision power control is needed.

Therefore, developing near-far resistant detectors by exploiting the structure of multi-access interference became the main issue in multiuser detection. The optimum receiver proposed by Verdu [1] has the best possible performance achievable in Gaussian noise channels. However, the performance comes at the expense of the exponential complexity in the number of users, and the knowledge of the received amplitudes, signature waveforms and timing of all users, which are usually not fixed and known in advance.

To greatly reduce the complexity of the optimum receiver with little trade off on performance, several suboptimum receivers have been proposed. These establish the basic structures for receivers proposed later. Notable among them are the decorrelating detector of Lupas and Verdu [2] [3]; the multistage detector of Varanasi and

Aazhang [4] [5]; the decision-feedback multiuser detectors of Duel-Hallen [6]; and the suboptimum detectors of Xie, Rushforth and Short [7] [8].

However, all these receivers still need the knowledge of the received amplitudes, signature waveforms and timing of all users. On the other hand, the adaptive detectors eliminate the need for the knowledge of some of the parameters. Spurred by their applications in mobile communications, where some of the parameters are usually not fixed, adaptive multiuser detection has roused a lot of interest in the multiuser detection area. A comprehensive introduction to various adaptive detectors can be found in [9]. All of them belong to one of two groups: the adaptive detection with training and without training.

The first group requires training sequences as the reference in the adaptation. This includes all the linear minimum mean-square error (MMSE) detectors, such as the suboptimum detector proposed by Xie, Short and Rushforth [8] and the adaptive receiver proposed by Rapajic and Vucetic [10]. The drawback of the detectors in this group is that in the asynchronous channel, where the interferers arrive and leave asynchronously, the sudden coming or going of an interference may result in the need for a new training sequence and the data transmission of the desired user has to be interrupted frequently to transmit the new training sequence.

The adaptive detectors that do not require training sequences are more practical in implementation. Among them are the blind multiuser detector by Honig [11] and the blind self-tuning maximum likelihood sequence estimator of Paris [12].

The receiver scheme investigated in this thesis has linear (in the number of users) complexity and is near-far resistant. But its most important features are that it is adaptive and it requires neither the knowledge of the received amplitude of any user nor training sequences. Thus, high precision power control and power estimation are not necessary and the receiver can also adjust itself quickly to changes in the

power of the users. This is essential to mobile communications, where the power of users keeps changing.

The synchronous version of the detector was proposed by Z. Siveski, Y. Bar-Ness and D.W. Chen [13] and the convergence and stability analysis was given by B. Zhu, N. Ansari, Z. Siveski and Y. Bar-Ness [14]. The generalization of it to the asynchronous case was presented by Z. Siveski, L. Zhong and Y. Bar-Ness [15]. The comprehensive version of the paper, including the convergence analysis, is enclosed in the thesis.

The structure of the system and mathematical model of it are shown in Chapter 2. Chapter 3 formulates the error probability of the decorrelator used at the first stage of the system with a new idea. The singularity problem associated with it is also discussed. The updating rule of the weights at the second stage, which optimize the output signal-to-noise-plus-interference ratio (SNIR), is investigated in Chapter 4. The convergence of the weights has been proved and their steady state values are given. Simulation results showing the transient behavior of the weights are also included. In Chaper 5, the error performance at the output of the detector is evaluated and shown to have superior performance to the conventional receiver and decorrelator in a scenario of practical interest.

# CHAPTER 2

## SYSTEM MODEL

The structure of the system is shown below.

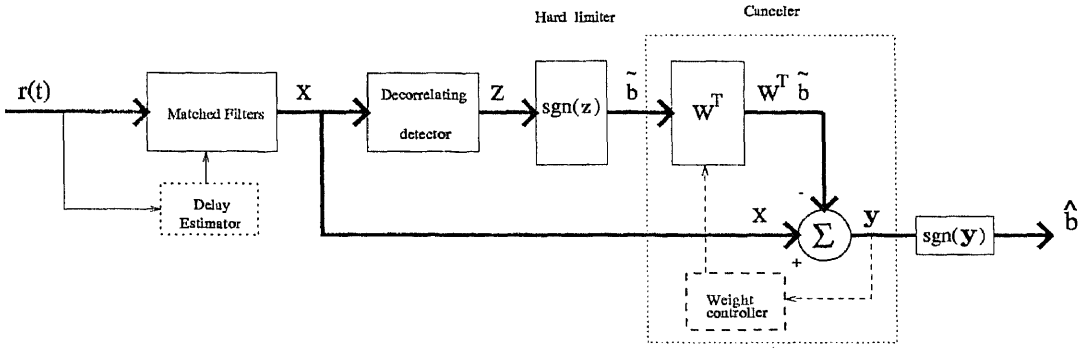


**Figure 2.1** System structure

In a multiuser environment, $K$ users share the same channel with the unit energy signature waveform $s_k(t)$, $k = 1, \ldots K$ of duration $T$, assigned to each of them. The information bits $b_k(i) \in \{\pm 1\}$ for the symbol interval $i$ have the same duration $T$. The waveform $r(t)$ at the input of the receiver, which has a bank of matched filters as its front end, is expressed as:

$$r(t) = \sum_{k=1}^{K} \sum_{i} b_k(i) \sqrt{a_k} s_k(t - iT - \tau_k) + n(t),$$

where $n(t)$ is a zero-mean, white Gaussian noise with the two-sided power spectral density $N_0/2$, and $a_k$ and $\tau_k$ are the received energy and relative delay for user $k$, respectively. While it is assumed that precise relative delay estimates are available for all users, their amplitudes are considered to be unknown to the receiver.

Without loss of generality, the attention will be on detection of bit $i$ of user 1, which is taken as the reference in time. It will be assumed that $0 = \tau_1 < \tau_2 < \ldots <$

$\tau_K < T$. The sampled output of the matched filter for user 1 is then:

$$x_1(i) = \sqrt{a_1}b_1(i) + \sum_{k=2}^{K} \sqrt{a_k}\left[\rho_{k1}b_k(i-1) + \rho_{1k}b_k(i)\right] + n_1(i).$$

The normalized partial cross-correlations for $k = 2, \ldots, K$ are:

$$\rho_{k1} = \int_0^T s_1(t)s_k(t+T-\tau_k)dt \quad \text{and} \quad \rho_{1k} = \int_0^T s_1(t)s_k(t-\tau_k)dt.$$

Also, $n_1(i) = \int_0^T n(t)s_1(t)dt$ is a zero-mean Gaussian random variable with variance $N_0/2$. Using the vector notations where $\boldsymbol{\rho}_1 = [\rho_{21}, \ldots, \rho_{K1}, \rho_{12}, \ldots, \rho_{1K}]^T$, $\boldsymbol{b}_1(i) = [b_2(i-1), \ldots, b_K(i-1), b_2(i), \ldots, b_K(i)]^T$, $\boldsymbol{A}_* = diag[\sqrt{a_2}, \ldots, \sqrt{a_K}]$, and $\boldsymbol{A}_1 = \begin{bmatrix} \boldsymbol{A}_* & \boldsymbol{0} \\ \boldsymbol{0} & \boldsymbol{A}_* \end{bmatrix}$, the matched filter output is:

$$x_1(i) = \sqrt{a_1}b_1(i) + \boldsymbol{\rho}_1^T\boldsymbol{A}_1\boldsymbol{b}_1(i) + n_1(i). \tag{2.1}$$

The multistage detector forms an estimate of the multiuser interference as the weighted vector of tentative decisions on symbols that interfere with $b_1(i)$ directly, and subtracts it from the matched filter output. The final decision statistics $y_1(i)$ and the corresponding final decision for bit $i$ of user 1 are:

$$y_1(i) = x_1(i) - \boldsymbol{w}_1^T(i)\tilde{\boldsymbol{b}}_1(i) \qquad \text{and} \qquad \hat{\mathrm{b}}_1(\mathrm{i}) = \mathrm{sgn}(\mathrm{y}_1(\mathrm{i})), \tag{2.2}$$

where $\boldsymbol{w}_1(i) = [w_{21}, \ldots, w_{K1}, w_{12}, \ldots, w_{1K}]^T$ are the corresponding weights, and $\tilde{\boldsymbol{b}}_1(i) = [\tilde{b}_2(i-1), \ldots, \tilde{b}_K(i-1), \tilde{b}_2(i), \ldots, \tilde{b}_K(i)]^T$ is the vector of tentative decisions affecting bit $i$ of user 1.

In this thesis, one-shot decorrelated tentative decision statistics are considered. The vector of the decorrelator outputs and the corresponding tentative decisions affecting bit $i$ of user 1 are:

$$\boldsymbol{z}_1(i) = \boldsymbol{A}_1\boldsymbol{b}_1(i) + \boldsymbol{\xi}_1(i) \qquad \text{and} \qquad \tilde{\boldsymbol{b}}_1(i) = \mathrm{sgn}(\boldsymbol{z}_1(i)) \tag{2.3}$$

where $\boldsymbol{\xi}_1(i) = [\xi_2(i-1), \ldots, \xi_K(i-1), \xi_2(i), \ldots, \xi_K(i)]^T$ is a zero-mean Gaussian vector having the covariance matrix $\boldsymbol{\Xi}_1$.

# CHAPTER 3

# DECORRELATOR

## 3.1 Error Probability at the Output of the Decorrelator

Let us consider each symbol interval separately and take bit $i$ of user 1 as the reference in time. Assuming without loss of generality that $0 = \tau_1 < \tau_2 < \ldots < \tau_K < T$, bit $i$ of user 1, which occupies the interval $[0, T]$, overlaps with bit $i-1$ of user $k$, $k = 2, 3, \ldots, K$ over the block $[0, \tau_2]$, with bit $i$ of user 2, bit $i-1$ of user $k$, $k = 3, 4, \ldots, K$ over the block $[\tau_2, \tau_3]$, ..., and with bit $i$ of user $k$, $k = 2, 3, \ldots, K$ over the block $[\tau_K, T]$. We can view the situation in each block as a $K$-user synchronous channel with unit-energy signature waveforms $\bar{s}_k^{bj}(t) = s_k^{bj}(t)/\sqrt{e_{bj}}$ $k, j = 1, 2, \ldots, K$, where

$$s_k^{bj}(t) = \begin{cases} s_k(t + \beta_{kj}T - \tau_k), & \tau_j < t < \tau_{j+1} \\ 0, & otherwise, \end{cases} \qquad \beta_{kj} = \begin{cases} 1, & j < k \\ 0, & otherwise \end{cases}$$

and

$$e_{bj} = \int_{\tau_j}^{\tau_{j+1}} s_k(t + \beta_{kj}T - \tau_k)^2 dt = \int_0^T s_k^{bj}(t)^2 dt, \qquad \forall k \in (1, 2, \ldots, K)$$

is the partial energy of the signals over the block $[\tau_j, \tau_{j+1}]$. The situations are illustrated in Figure 3.1 below.

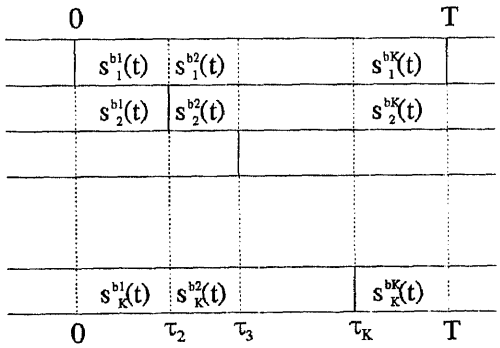


**Figure 3.1** The situations in the i-th symbol interval of user 1

Therefore, results derived for the synchronous case [13] can be used here. Without loss of generality, we focus our attention on the first block $[0, \tau_2]$. The received signal $r(t)$ in this block can be expressed as:

$$r(t) = \sqrt{e_{b1}}[\sqrt{a_1}b_1(i)\bar{s}_1^{b1}(t) + \sum_{k=2}^{K}\sqrt{a_k}b_k(i-1)\bar{s}_k^{b1}(t)] + n(t).$$

To simplify the notations, the index i will be omitted where no confusion will be caused.

The sampled outputs of the bank of matched filters (sampled at $t = \tau_2$ ) will be:

$$\boldsymbol{x}_{b1} = \sqrt{e_{b1}}\boldsymbol{\mathcal{P}}_{b1}\boldsymbol{A}\boldsymbol{b}_{b1} + \boldsymbol{n}_{b1},$$

where $\boldsymbol{x}_{b1} = [x_{1b1}, x_{2b1}, \ldots, x_{Kb1}]^T$, $\boldsymbol{b}_{b1} = [b_1(i), b_2(i-1), \ldots, b_K(i-1)]^T$, $\boldsymbol{A} = diag[\sqrt{a_1}, \sqrt{a_2}, \ldots, \sqrt{a_K}]$ and the $(m,l)$th element of the matrix $\boldsymbol{\mathcal{P}}_{b1}$ is defined as:

$$\rho_{b1ml} = \frac{1}{e_{b1}}\int_0^T s_m^{b1}(t)s_l^{b1}(t)dt \qquad m, l \in (1, 2, \ldots, K).$$

Obviously, $\boldsymbol{\mathcal{P}}_{b1}$ is a symmetric matrix with diagonal elements equal to 1. $\boldsymbol{n}_{b1} = [n_{1b1}, n_{2b1}, \ldots, n_{Kb1}]^T$ is the filtered Guassian noise random vector with covariance $E\{\boldsymbol{n}_{b1}\boldsymbol{n}_{b1}^T\} = \frac{N_0}{2}\boldsymbol{\mathcal{P}}_{b1}$.

The outputs of the decorrelator for the block $[0, \tau_2]$ are given as:

$$\boldsymbol{z}_{b1} = \boldsymbol{\mathcal{P}}_{b1}^{-1}\boldsymbol{x}_{b1} = \sqrt{e_{b1}}\boldsymbol{A}\boldsymbol{b}_{b1} + \boldsymbol{\xi}_{b1},$$

where $\boldsymbol{z}_{b1} = [z_{1b1}, z_{2b1}, \ldots, z_{Kb1}]^T$, $\boldsymbol{\xi}_{b1} = [\xi_{1b1}, \xi_{2b1}, \ldots, \xi_{Kb1}]^T = \boldsymbol{\mathcal{P}}_{b1}^{-1}\boldsymbol{n}_{b1} = \boldsymbol{\Gamma}_{b1}\boldsymbol{n}_{b1}$ and $\boldsymbol{\Gamma}_{b1} = \boldsymbol{\mathcal{P}}_{b1}^{-1}$.

Since $E\{\boldsymbol{n}_{b1}\boldsymbol{n}_{b1}^T\} = \frac{N_0}{2}\boldsymbol{\mathcal{P}}_{b1}$ and $\boldsymbol{\Gamma}_{b1} = \boldsymbol{\mathcal{P}}_{b1}^{-1}$,

$$E\{\boldsymbol{\xi}_{b1}\boldsymbol{\xi}_{b1}^T\} = E\{(\boldsymbol{\Gamma}_{b1}\boldsymbol{n}_{b1})(\boldsymbol{\Gamma}_{b1}\boldsymbol{n}_{b1})^T\} = \boldsymbol{\Gamma}_{b1}E\{\boldsymbol{n}_{b1}\boldsymbol{n}_{b1}^T\}\boldsymbol{\Gamma}_{b1}^T = \frac{N_0}{2}\boldsymbol{\Gamma}_{b1}.$$

For user 1, we have

$$z_{1b1} = \sqrt{e_{b1}}\sqrt{a_1}b_1(i) + \xi_{1b1},$$

and

$$Var(\xi_{1b1}) = \frac{N_0}{2}\gamma_{b111},$$

where $\gamma_{b111}$ is the first diagonal element of the matrix $\boldsymbol{\Gamma}_{b1}$.

Similarly, for the kth block $[\tau_k, \tau_{k+1}]$ of user 1, we will have

$$z_{1bk} = \sqrt{e_{bk}}\sqrt{a_1}b_1(i) + \xi_{1bk}, \tag{3.1}$$

and

$$Var(\xi_{1bk}) = \frac{N_0}{2}\gamma_{bk11} \qquad k = 1, 2, \ldots, K, \tag{3.2}$$

where $\gamma_{bk11}$ is the first diagonal element of the matrix $\boldsymbol{\Gamma}_{bk}$, while $\boldsymbol{\Gamma}_{bk} = \boldsymbol{\mathcal{P}}_{bk}^{-1}$ and the $(m, l)$th elememt of the matrix $\boldsymbol{\mathcal{P}}_{bk}$ is defined as:

$$\rho_{bkml} = \frac{1}{e_{bk}}\int_0^T s_m^{bk}(t)s_l^{bk}(t)dt \qquad k, m, l \in (1, 2, \ldots, K).$$

The decorrelator outputs for the i-th symbol interval can be constructed as the weighted sum of those of the $K$ non-overlapping blocks $[0, \tau_2], [\tau_2, \tau_3], \ldots, [\tau_K, T]$. Without loss of generality, attention is focused on user 1 only.

The decorrelator outputs for the i-th symbol interval of user 1 are:

$$z_1 = \boldsymbol{c}_1^T \boldsymbol{z}_{1b} = \sum_{k=1}^{K} c_{1bk}z_{1bk}, \tag{3.3}$$

where $\boldsymbol{z}_{1b} = [z_{1b1}, z_{1b2}, \ldots, z_{1bK}]^T$, and the weights $\boldsymbol{c}_1 = [c_{1b1}, c_{1b2}, \ldots, c_{1bK}]^T$. The weights are selected in such a way that the error probability at the output of the decorrelator for user 1 will be minimized. The derivation of such optimum weights will be shown in the next section. The results are:

$$c_{1bk} = \frac{\sqrt{e_{bk}}}{\gamma_{bk11}}\Gamma_{11} \qquad k = 1, 2, \ldots, K, \tag{3.4}$$

where

$$\Gamma_{11} = \frac{1}{\sum_{k=1}^{K}\frac{e_{bk}}{\gamma_{bk11}}},$$

which can be regarded as the parallel connections of the $\gamma_{bk11}$ of each block weighted by the partial energy of that block. $\Gamma_{11}$ is an important parameter of the decorrelator. As will be shown later, it is related to the variance of the noise at the output of the decorrelator and the asymptotic efficiency of the decorrelator.

Substituting the optimum values of the weights into Eq.(3.3), and using the conclusion in Eq.(3.1), we will have:

$$\begin{aligned} z_1 &= \sum_{k=1}^{K} \frac{\sqrt{e_{bk}}}{\gamma_{bk11}} \Gamma_{11} z_{1bk} \\ &= \sum_{k=1}^{K} \frac{\sqrt{e_{bk}}}{\gamma_{bk11}} \Gamma_{11} [\sqrt{e_{bk}} \sqrt{a_1} b_1(i) + \xi_{1bk}] \\ &= \left[ \sum_{k=1}^{K} \frac{e_{bk}}{\gamma_{bk11}} \right] \Gamma_{11} \sqrt{a_1} b_1(i) + \sum_{k=1}^{K} \frac{\sqrt{e_{bk}}}{\gamma_{bk11}} \Gamma_{11} \xi_{1bk} \\ &= \sqrt{a_1} b_1(i) + \xi_1, \end{aligned} \tag{3.5}$$

where $\xi_1 = \sum_{k=1}^{K} \frac{\sqrt{e_{bk}}}{\gamma_{bk11}} \Gamma_{11} \xi_{1bk}$ and since $\xi_{1bk}, \quad k = 1, 2, \ldots, K$ belong to $K$ non-verlapping blocks, they are uncorrelated with each other, thus we have:

$$\begin{aligned} Var(\xi_1) &= \Gamma_{11}^2 \sum_{k=1}^{K} \frac{e_{bk}}{\gamma_{bk11}^2} Var(\xi_{1bk}) \\ &= \frac{N_0}{2} \Gamma_{11}^2 \sum_{k=1}^{K} \frac{e_{bk}}{\gamma_{bk11}} \\ &= \frac{N_0}{2} \Gamma_{11}. \end{aligned} \tag{3.6}$$

The tentative decision at the output of decorrelator for user 1 is $\tilde{b}_1(i) = \text{sgn}(z_1(i))$.

The corresponding error probability is evaluated as:

$$\begin{aligned} Pr\{\tilde{b}_1(i) \text{ in error}\} &= Pr\{\tilde{b}_1(i) = 1 | b_1(i) = -1\} Pr\{b_1(i) = -1\} \\ &+ Pr\{\tilde{b}_1(i) = -1 | b_1(i) = 1\} Pr\{b_1(i) = 1\}. \end{aligned}$$

Since the channel is a Binary Symmetric Channel (BSC),

$$Pr\{\tilde{b}_1(i) = 1 | b_1(i) = -1\} = Pr\{\tilde{b}_1(i) = -1 | b_1(i) = 1\},$$

and $Pr\{b_1(i)=1\} = Pr\{b_1(i)=-1\} = \frac{1}{2}$.

$$\begin{aligned} Pr\{\tilde{b}_1(i) \text{ in error}\} &= Pr\{\tilde{b}_1(i)=1 | b_1(i)=-1\} \\ &= Pr\{z_1(i)>0 | b_1(i)=-1\} \\ &= Pr\{-\sqrt{a_1}+\xi_1>0\} \\ &= Pr\{\xi_1>\sqrt{a_1}\} \\ &= Q\left(\sqrt{\frac{a_1}{Var(\xi_1)}}\right) \\ &= Q\left(\sqrt{\frac{a_1}{\frac{N_0}{2}\Gamma_{11}}}\right). \end{aligned} \tag{3.7}$$

From the above equation, it is obvious that the asymptotic efficiency of the decorrelator is:

$$\eta_1^d = \frac{1}{\Gamma_{11}} = \sum_{k=1}^{K} \frac{e_{bk}}{\gamma_{bk11}}. \tag{3.8}$$

To illustrate the above derivations, the two-user case will be described in detail in Appendix A.

We can specify the system structure in more detail using the idea mentioned above. This diagram is shown in Appendix E. One can see from the diagram that altogether $K^2$ of matched filters are used in the receiver of K users, so only K matched filters are needed for each user. The complexity of the receiver, which is mainly measured by the number of matched filters used, is linear with the number of users.

## 3.2 Optimum Weights

From Eq.(3.1) and Eq.(3.3), we have:

$$\begin{aligned} z_1 &= \sum_{k=1}^{K} c_{1bk}[\sqrt{e_{bk}}\sqrt{a_1}b_1(i) + \xi_{1bk}] \\ &= \left[\sum_{k=1}^{K} c_{1bk}\sqrt{e_{bk}}\right]\sqrt{a_1}b_1(i) + \sum_{k=1}^{K} c_{1bk}\xi_{1bk} \\ &= \left[\sum_{k=1}^{K} c_{1bk}\sqrt{e_{bk}}\right]\sqrt{a_1}b_1(i) + \xi_1, \end{aligned} \tag{3.9}$$

where $\xi_1 = \sum_{k=1}^{K} c_{1bk}\xi_{1bk}$, and

$$\begin{aligned} Var(\xi_1) &= \sum_{k=1}^{K} c_{1bk}^2 Var(\xi_{1bk}) \\ &= \sum_{k=1}^{K} c_{1bk}^2 \frac{N_0}{2}\gamma_{bk11} \\ &= \frac{N_0}{2}\sum_{k=1}^{K} c_{1bk}^2 \gamma_{bk11}. \end{aligned} \tag{3.10}$$

The error probability at the output of the decorrelator for user 1 is evaluated as follows:

$$\begin{aligned} Pr\{\tilde{b}_1(i) \text{ in error}\} &= Pr\{\tilde{b}_1(i) = 1 | b_1(i) = -1\} \\ &= Pr\{z_1(i) > 0 | b_1(i) = -1\} \\ &= Pr\{-\left[\sum_{k=1}^{K} c_{1bk}\sqrt{e_{bk}}\right]\sqrt{a_1} + \xi_1 > 0\} \\ &= Pr\{\xi_1 > \left[\sum_{k=1}^{K} c_{1bk}\sqrt{e_{bk}}\right]\sqrt{a_1}\} \\ &= Q\left(\frac{\left[\sum_{k=1}^{K} c_{1bk}\sqrt{e_{bk}}\right]\sqrt{a_1}}{\sqrt{Var(\xi_1)}}\right) \\ &= Q\left(\sqrt{\frac{a_1}{\frac{N_0}{2}}}\frac{\sum_{k=1}^{K} c_{1bk}\sqrt{e_{bk}}}{\sqrt{\sum_{k=1}^{K} c_{1bk}^2\gamma_{bk11}}}\right). \end{aligned} \tag{3.11}$$

Define

$$L = \frac{\sum_{k=1}^{K} c_{1bk}\sqrt{e_{bk}}}{\sqrt{\sum_{k=1}^{K} c_{1bk}^2\gamma_{bk11}}}.$$

It is obvious that by maximizing L, the error probability at the output of the decorrelator for user 1 will be minimized.

The optimum weights are evaluated as follows: $\forall j \in (1, 2, \ldots, K)$

$$\frac{\partial L}{\partial c_{1bj}} = \frac{\sqrt{\sum_{k=1}^{K} c_{1bk}^2\gamma_{bk11}}\sqrt{e_{bj}} - \sum_{k=1}^{K} c_{1bk}\sqrt{e_{bk}}\frac{1}{2}\frac{1}{\sqrt{\sum_{k=1}^{K} c_{1bk}^2\gamma_{bk11}}}2c_{1bj}\gamma_{bj11}}{\sum_{k=1}^{K} c_{1bk}^2\gamma_{bk11}},$$

so the optimum weights will be the ones that satisfy the equations $\frac{\partial L}{\partial c_{1bj}} = 0, \quad j = 1, 2, \ldots, K$, which are true if and only if

$$\sqrt{\sum_{k=1}^{K} c_{1bk}^2\gamma_{bk11}}\sqrt{e_{bj}} - \sum_{k=1}^{K} c_{1bk}\sqrt{e_{bk}}\frac{1}{2}\frac{1}{\sqrt{\sum_{k=1}^{K} c_{1bk}^2\gamma_{bk11}}}2c_{1bj}\gamma_{bj11} = 0,$$

which can be rewritten as:

$$\sum_{k=1}^{K} c_{1bk}[c_{1bk}\gamma_{bk11}\sqrt{e_{bj}} - c_{1bj}\gamma_{bj11}\sqrt{e_{bk}}\,] = 0,$$

and which will be satisfied if

$$c_{1bk}\gamma_{bk11}\sqrt{e_{bj}} = c_{1bj}\gamma_{bj11}\sqrt{e_{bk}} \qquad \forall j,k \in (1,2,\ldots,K)$$

or

$$c_{1bk}\frac{\gamma_{bk11}}{\sqrt{e_{bk}}} = c_{1bj}\frac{\gamma_{bj11}}{\sqrt{e_{bj}}} \qquad \forall j,k \in (1,2,\ldots,K).$$

If we set

$$c_{1bk}\frac{\gamma_{bk11}}{\sqrt{e_{bk}}} = \alpha \qquad k = 1,2,\ldots,K,$$

where $\alpha$ is an arbitrary non-zero constant, the above equation will be satisfied.

The value of $\alpha$ has no effect on that of $L$ and therefore the error probability, and for sake of convenience, $\alpha = \Gamma_{11}$ is used in the thesis to make the $\sum_{k=1}^{K} c_{1bk}\sqrt{e_{bk}}$ in Eq.(3.9) equal to 1 and simplify the equation.

So the optimum weights will be:

$$c_{1bk} = \frac{\sqrt{e_{bk}}}{\gamma_{bk11}}\Gamma_{11} \qquad k = 1,2,\ldots,K. \tag{3.12}$$

### 3.3 Singularity Problem

Let us look at the synchronous case first. In this case, the outputs of the decorrelator [2] are given as:

$$\boldsymbol{z} = \boldsymbol{P}^{-1}\boldsymbol{x},$$

where $\boldsymbol{z}$ and $\boldsymbol{x}$ are the outputs of the decorrelator and matched filters correspondingly, and $\boldsymbol{P}$ is the cross-correlation matrix of the system. It is obvious that when $\boldsymbol{P}$ is singular, the decorrelator doesn't work at all.

Therefore the asynchronous case, which can be regarded as K synchronous channels, has the same problem. For each block where the cross-correlation matrix

is singular, the corresponding weight can be set to zero so that only those blocks where the decorrelator works normally will contribute to the overall performance in the entire symbol interval. So if only some blocks of the symbol interval have the singularities, we can still make a decorrelating tentative estimate for that symbol interval.

If all the blocks in one symbol interval have the singularities at the same time, it is obvious that we can't get any decorrelating tentative estimate for all users. In this case, all weights will be set to zero, and $z_k = 0, \quad k = 1, 2, \ldots, K$, i.e. there would be neither data nor noise. From the view of our two-stage detector, it is like disconnecting the decorrelating estimates for all users. So the final output at the second stage of our detector will be conventional.

We define $\tau = [\tau_1, \tau_2, \ldots, \tau_K]^T$ when all the blocks in one symbol interval have the singularities at the same time as the singular point. One can claim that the probability for such singular points are near zero since $\tau$ is uniformly distributed over $[0, T]^K$ and those singular points are only a finite number of points in such a continuous space. But there are two types of singular points. One is "continuous", the other is not. For a "continuous" singular point, when $\tau$ is very close to the singular point, the corresponding performance will also be very close to that of the singular point. If this is the case, the probability for the system to have near-conventional performance will not be small and since the error probabilities in these regions are generally high, their impact on the average error probability of the system can not be neglected.

To solve the problem, we can either use signature sequences with larger lengths (one can use signature sequences with more chips for one symbol interval, or for more than one symbol intervals while keeping the number of chips per symbol interval the same as before), or use the L-shot decorrelator ($L > 1$) to reduce the probability of singularity. To eliminate the singularity problem completely, one should replace the

inverse operation of the cross-correlation matrix in the decorrelating detector with singular decomposition. And from the viewpoint of the control system, the cause of singularity is that the data of some users is unobservable. Therefore, adding more estimates at the first stage (such as more matched filters) will help to recover those data vanishing due to singularity.

Before we conclude the chapter, we will illustrate the aforementioned singularity problem with some numerical results derived from accurate computation of the error probability. At first, a three-dimensional graph of the error probability distribution of the decorrelator over the relative delays $\tau_2$ and $\tau_3$ will be shown to give one an overall picture about how the relative delays influence the error probability of the decorrelator. One can see from the picture that there are a lot of singular points, some of which are "continuous", having an obvious impact on the performance of the decorrelator (which is usually measured by its worst and averge error probability). Actually, even though most of the points are below $Pe_1 = 10^{-4}$, the average error probability is $9.377649 \times 10^{-4}$.

To show the behavior of the singular points more clearly, cuts of the above picture at $\tau_3 = 2/7T$ and $\tau_3 = 3/7T$ are taken in Figure 3.3 and Figure 3.4. Two types of singular points (a "continuous" one and a "discontinuous" one ) are shown.

The impact of decorrelating estimates with singularities on the second stage of the proposed detector is shown in Figure 3.5 for the cut taken at $\tau_3 = 5/7T$. The error probability curve of the proposed detector is shown for the case of the decorrelator and the conventional single-user detector. It can be seen that when both interfering users have singularities, the error probabilty of the proposed detector is equal to that of the conventinal single-user detector.

All these figures are for the three-user case and under the condition that $SNR_i = 12dB, \quad i = 1, 2, 3.$

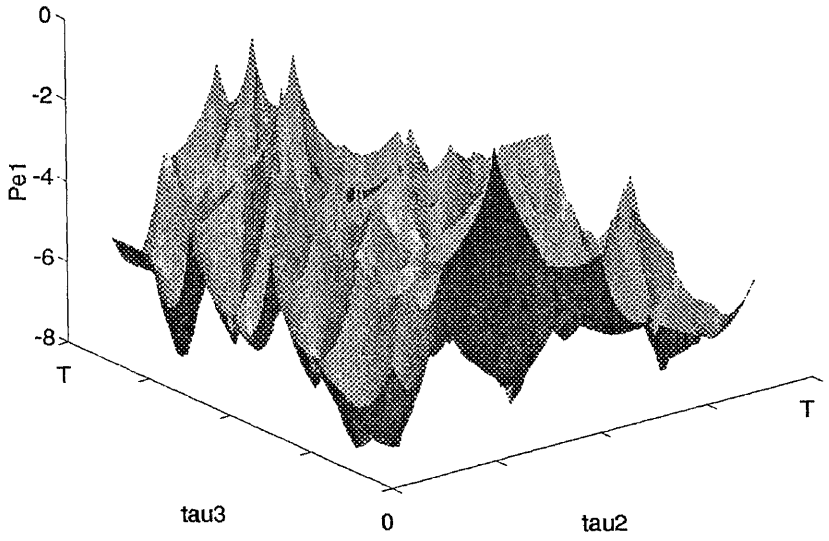


Figure 3.2 Distribution of the error probability of the decorrelator over $\tau_2$ and $\tau_3$

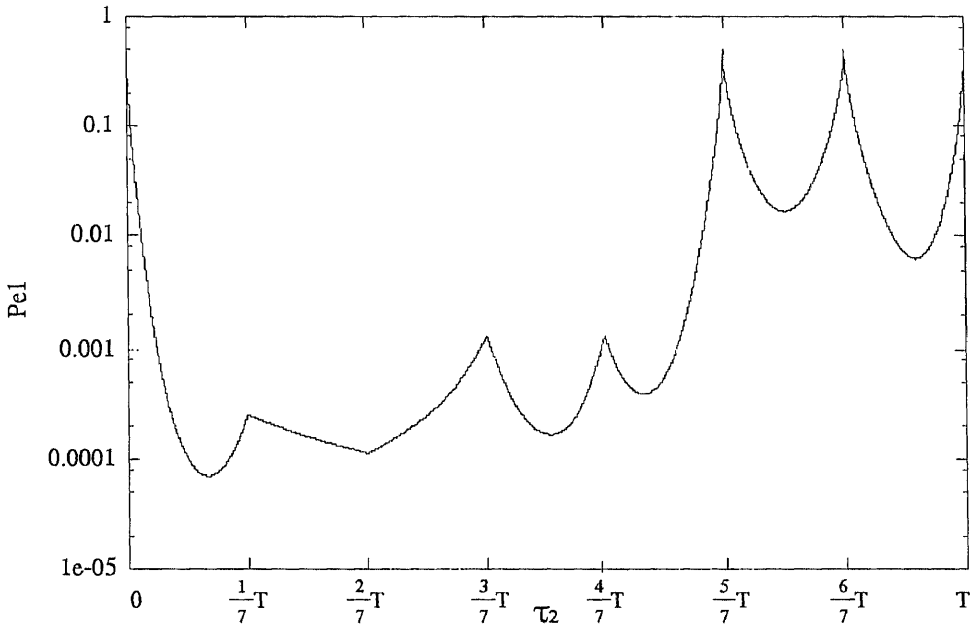


**Figure 3.3** "Continuous" singular points for $\tau_3 = 2/7T$

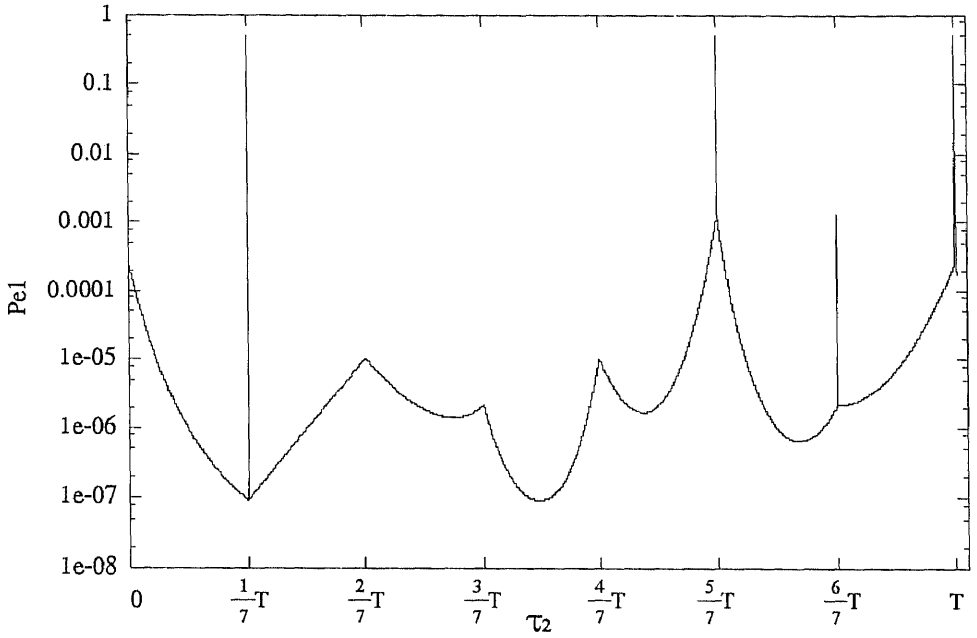


**Figure 3.4** "Discontinuous" singular points for $\tau_3 = 3/7T$

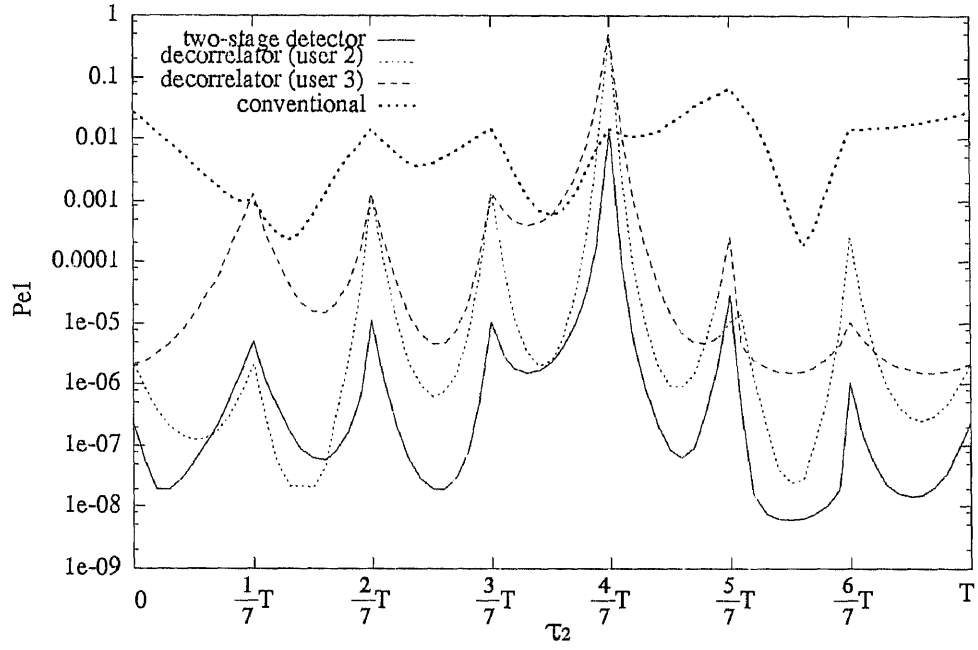


**Figure 3.5** The behavior of the "continuous" singular points for $\tau_3 = 5/7T$

# CHAPTER 4

# ADAPTIVE WEIGHTS

## 4.1 The Updating Rule

From Eq.(2.1) and Eq.(2.2), the output of The multistage detector for user 1 can be expressed as:

$$\begin{aligned} y_1 &= x_1 - \boldsymbol{w}_1^T \tilde{\boldsymbol{b}}_1 \\ &= \sqrt{a_1} b_1(i) + \rho_1^T \boldsymbol{A}_1 \boldsymbol{b}_1 - \boldsymbol{w}_1^T \tilde{\boldsymbol{b}}_1 + n_1. \end{aligned}$$

The output noise-plus-interference power can be obtained by subtracting the output signal power $a_1$ from the output power $E\{y_1^2\}$. Thus, the SNIR, defined as the ratio between the output signal power and the sum of the output noise and interference power, can be calculated from:

$$SNIR = \frac{a_1}{E\{y_1^2\} - a_1}. \tag{4.1}$$

It is obvious that the output signal-to-noise-plus-interference ratio SNIR, which is a good measurement of the performance of the spread spectrum system, will be maximized when the weights are selected in such a way that the ouput power $E\{y_1^2\}$ is minimized.

In this thesis, the steepest descent algorithm is used to minimize the ouput power $E\{y_1^2\}$. So the updating rule of the weights will be:

$$\begin{aligned} \boldsymbol{w}_1(i+1) &= \boldsymbol{w}_1(i) - \frac{\mu}{2} \frac{\partial}{\partial \boldsymbol{w}_1(i)} E\{y_1^2(i)\} \\ &= \boldsymbol{w}_1(i) + \mu E\{y_1(i) \tilde{\boldsymbol{b}}_1(i)\} \qquad (4.2) \\ &= \boldsymbol{w}_1(i) + \mu E\{[x_1(i) - \tilde{\boldsymbol{b}}_1^T(i) \boldsymbol{w}_1(i)] \tilde{\boldsymbol{b}}_1(i)\} \\ &= \boldsymbol{w}_1(i) + \mu E\{x_1(i) \tilde{\boldsymbol{b}}_1(i)\} - \mu E\{\tilde{\boldsymbol{b}}_1(i) \tilde{\boldsymbol{b}}_1^T(i)\} \boldsymbol{w}_1(i) \qquad (4.3) \\ &= [\boldsymbol{I} - \mu E\{\tilde{\boldsymbol{b}}_1(i) \tilde{\boldsymbol{b}}_1^T(i)\}] \boldsymbol{w}_1(i) + \mu E\{x_1(i) \tilde{\boldsymbol{b}}_1(i)\} \end{aligned}$$

$$= \boldsymbol{H}_1 \boldsymbol{w}_1(i) + \mu E\{x_1(i)\tilde{\boldsymbol{b}}_1(i)\} \tag{4.4}$$

where $\boldsymbol{H}_1 = \boldsymbol{I} - \mu E\{\tilde{\boldsymbol{b}}_1(i)\tilde{\boldsymbol{b}}_1^T(i)\}$ is a symmetric matrix with diagonal elements equal to $1-\mu$ (the two-user case is described in Appendix B).

## 4.2 Convergence and Stability Analysis

Let $\boldsymbol{\delta}_1(i) = \boldsymbol{w}_1^0 - \boldsymbol{w}_1(i)$, where $\boldsymbol{w}_1^0$ is the steady state of $\boldsymbol{w}_1(i)$. It follows from Eq.(4.4) that:

$$\boldsymbol{\delta}_1(i+1) = \boldsymbol{H}_1\boldsymbol{\delta}_1(i) = \boldsymbol{H}_1^{i+1}\boldsymbol{\delta}_1(0)$$

or

$$\boldsymbol{\delta}_1(i) = \boldsymbol{H}_1^i\boldsymbol{\delta}_1(0).$$

The weights converge if and only if

$$\lim_{i\to\infty} \boldsymbol{\delta}_1(i) = 0,$$

which is therefore equivalent to

$$\lim_{i\to\infty} \boldsymbol{H}_1^i = 0.$$

Since $\boldsymbol{H}_1$ is a symmetric matrix, there exists a real diagonal matrix $\boldsymbol{D}_1 = diag[\lambda_1, \lambda_2, \ldots, \lambda_{2(K-1)}]$, such that $\boldsymbol{H}_1 = \boldsymbol{Q}\boldsymbol{D}_1\boldsymbol{Q}^{-1}$. So $\lim_{i\to\infty}\boldsymbol{H}_1^i = 0$ is further equivalent to $\lim_{i\to\infty}\boldsymbol{D}_1^i = 0$, which is guaranteed by:

$$|\lambda_j| < 1, \quad j = 1, 2, \ldots, 2(K-1). \tag{4.5}$$

To relate $\lambda_j$ to $\mu$, we apply the Gershgorin theorem[1] to $\boldsymbol{H}_1$. For $\forall\lambda_j$, $j = 1, 2, \ldots, 2(K-1)$, there exists at least an m $\in (1, 2, \ldots, 2K-2)$ such that:

$$\begin{aligned} |\lambda_j - (1-\mu)| &= |\lambda_j - H_{mm}| \\ &\leq \sum_{m_0 \neq m} |\boldsymbol{H}_{m_0 m}| \\ &\leq 2(K-2)\mu e_{max}, \end{aligned}$$

[1] If $\boldsymbol{M}$ is a complex square matrix of order n with its element denoted as $m_{ij}$, every characteristic root of the complex matrix $\boldsymbol{M}$ lies in at least one of the n disks with centers $m_{ii}$, radii $r_i = \sum_{j=1, j\neq i}^{n} |m_{ij}|$. [16]

where $e_{max}$ is the maximum value of the absolute values of the off-diagonal elements of matrix $E\{\tilde{\boldsymbol{b}}_1(i)\tilde{\boldsymbol{b}}_1^T(i)\}$, and $E\{\tilde{b}_k(i)\tilde{b}_k(i-1)\} = 0, \quad k = 1, 2, \ldots, K$ are taken into account in the above derivation.

It follows that

$$\begin{aligned} |\lambda_j| &\leq |\lambda_j - (1-\mu)| + |1-\mu| \qquad j = 1, 2, \ldots, 2(K-1) \\ &\leq 2(K-2)\mu e_{max} + |1-\mu|, \end{aligned}$$

and if $0 < \mu < 1$,

$$\begin{aligned} |\lambda_j| &\leq 2(K-2)\mu e_{max} + 1 - \mu \qquad j = 1, 2, \ldots, 2(K-1) \\ &= 1 + \mu[2(K-2)e_{max} - 1]. \end{aligned} \tag{4.6}$$

It is obvious that when $0 < \mu < 1$ and $2(K-2)e_{max} < 1$,

$$|\lambda_j| < 1, \qquad j = 1, 2, \ldots, 2(K-1),$$

which guarantees the convergence of $\boldsymbol{w}_1$.

### 4.3 Steady State Values of the Weights

From Eq.(4.3), the steady state values of the weights are evaluated as follows:

$$\boldsymbol{w}_1^0 = \boldsymbol{w}_1^0 + \mu E\{x_1(i)\tilde{\boldsymbol{b}}_1(i)\} - \mu E\{\tilde{\boldsymbol{b}}_1(i)\tilde{\boldsymbol{b}}_1^T(i)\}\boldsymbol{w}_1^0,$$

thus

$$\boldsymbol{w}_1^0 = \left[E\{\tilde{\boldsymbol{b}}_1(i)\tilde{\boldsymbol{b}}_1^T(i)\}\right]^{-1} E\{x_1(i)\tilde{\boldsymbol{b}}_1(i)\}. \tag{4.7}$$

From the properties of the decorrelator, it is easy to show that $E\{n_1(i)\xi_k(i)\} = 0$, and $E\{n_1(i)\xi_k(i-1)\} = 0$, for $k \neq 1$, so the first of the two expectations above is:

$$E\{x_1(i)\tilde{\boldsymbol{b}}_1(i)\} = \boldsymbol{A}_1 E\{\boldsymbol{b}_1(i)\tilde{\boldsymbol{b}}_1^T(i)\}\boldsymbol{\rho}_1. \tag{4.8}$$

Therefore, the steady state values of the weights affecting the first output are:

$$\boldsymbol{w}_1^0 = \left[E\{\tilde{\boldsymbol{b}}_1(i)\tilde{\boldsymbol{b}}_1^T(i)\}\right]^{-1} \boldsymbol{A}_1 E\{\boldsymbol{b}_1(i)\tilde{\boldsymbol{b}}_1^T(i)\}\boldsymbol{\rho}_1. \tag{4.9}$$

The evaluation for the expectations in Eq.(4.9) are shown in Appendix D.

## 4.4 Simulation Results

In all the simulations, the signal-to-noise ratio for user k is defined as $SNR_k = a_k/N_0, \quad k = 1, 2, \ldots, K$. The expectations $E\{x_1(i)\tilde{\boldsymbol{b}}_1(i)\}$ and $E\{\tilde{\boldsymbol{b}}_1(i)\tilde{\boldsymbol{b}}_1(i)^T\}$ in the updating rule of the weights are approximated by moving average with sliding window. The flow chart of the simulation program is shown in Figure 4.7.

Figures 4.1 to 4.3 show results for the two-user case, with $\rho_{12} = 0.2$, $\rho_{21} = 0.6$, $e_1 = 0.4$ and $SNR_1 = 8dB$. The results for the three-user case are shown in Figures 4.4 to 4.6, where all three users' SNR's are fixed to 8dB, a condition unfavorable to the proposed two-stage detector. The signature waveforms and timing of all users are the same as those of Figure 5.5 for comparison.

Figure 4.1 shows the effect of the learning rate $\mu$ on the updating process of the weight $w_{21}$ for two-user case. It is clear that the larger the $\mu$ is, the faster the convergence will be, when the other parameters are the same. But larger undulation is expected for a larger $\mu$. These are also true for an arbitrary number of users, which are obvious from Eq.(4.2) and Eq.(4.6). The results for the three-user case are shown in Figure 4.4.

The ensemble behavior of the weight $w_{21}$ from 100 independent simulations is shown in Figure 4.2. Here, $\mu$ is chosen as 0.2. Results which account for three typical situations: strong interference, perfect power control and weak interference are included, where $SNR_2 = 12dB$, $8dB$, $2dB$ respectively. Note that the number of iterations required for the weight $w_{21}$ to reach steady state in all three cases is less than 50, demonstrating a very fast convergence. Figure 4.5 shows that this is also true for the three-user case and implicitly for an arbitrary number of users.

Finally, the transient behaviors of the system at the output for user 1 are shown for the two-user case in Figure 4.3 and for the three-user case in Figure 4.6. The results for each iteration are statistics from 50,000 independent simulations.

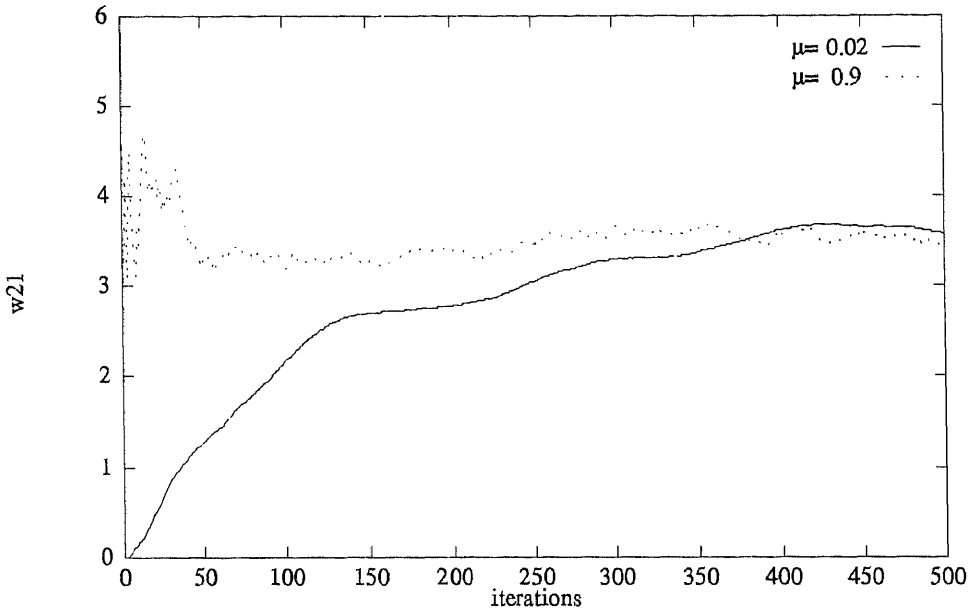


**Figure 4.1**: The effect of $\mu$ on the updating process of the weight $w_{21}$ with $SNR_1 = 8dB, SNR_2 = 12dB, \rho_{12} = 0.2, \rho_{21} = 0.6, e_1 = 0.4, K = 2$

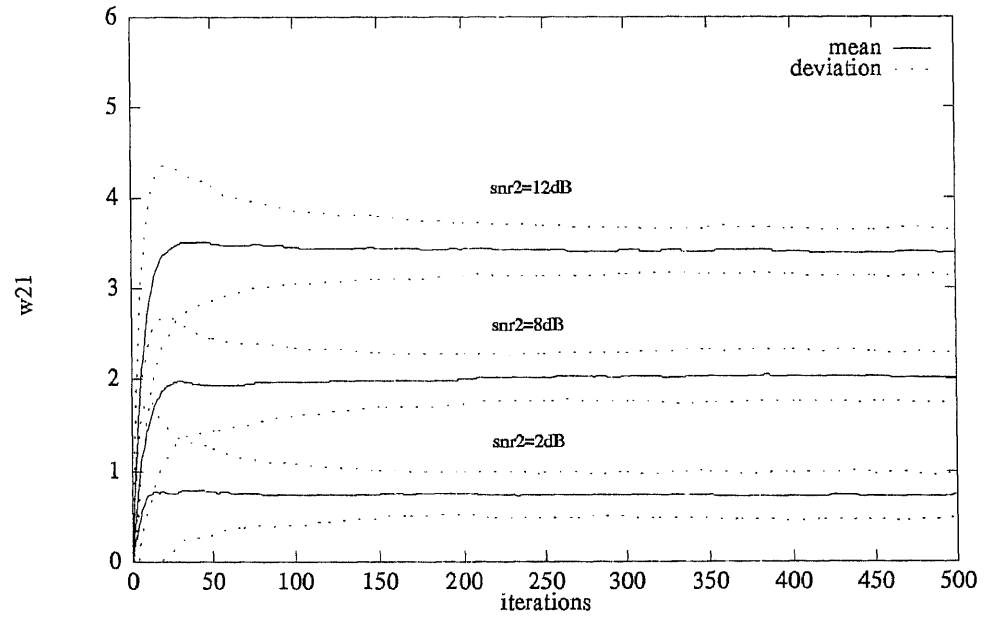


**Figure 4.2** The ensemble behavior of the weight $w_{21}$ in convergence with $\mu = 0.2$

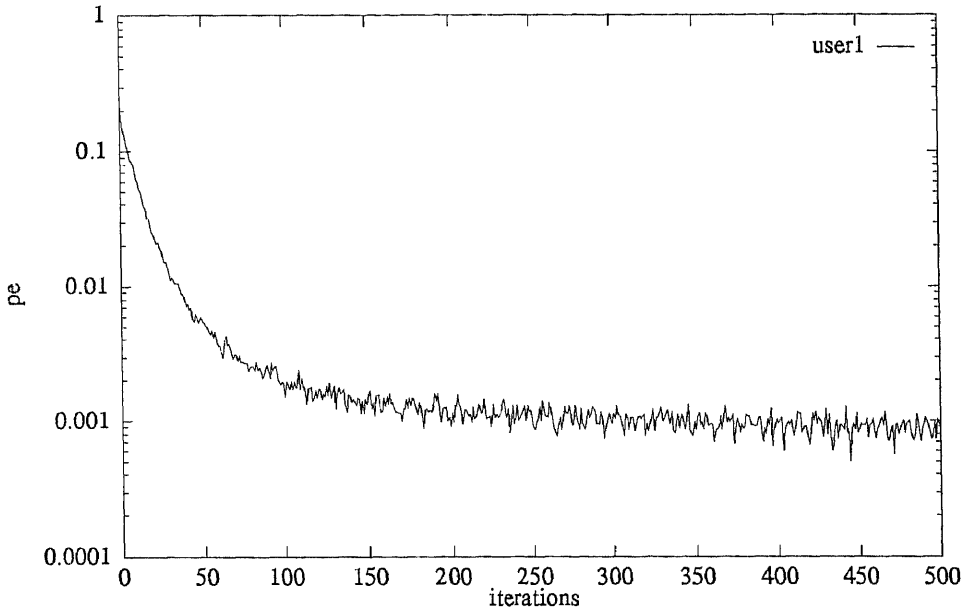


**Figure 4.3** The convergence of $Pe_1$ *with* $SNR_2 = 12dB$, $\mu = 0.2$ *and* $K = 2$

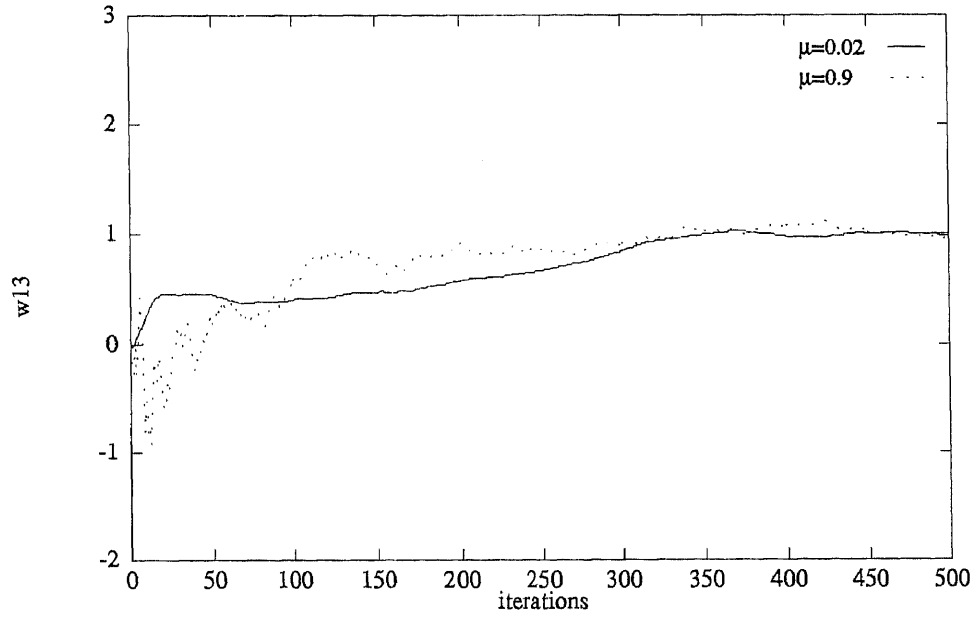


**Figure 4.4**: The effect of $\mu$ on the updating process of the weight $w_{13}$ with $SNR_1 = SNR_2 = SNR_3 = 8dB$, $\tau_2 = T/7$, $\tau_3 = 5T/7$ *and* $K = 3$

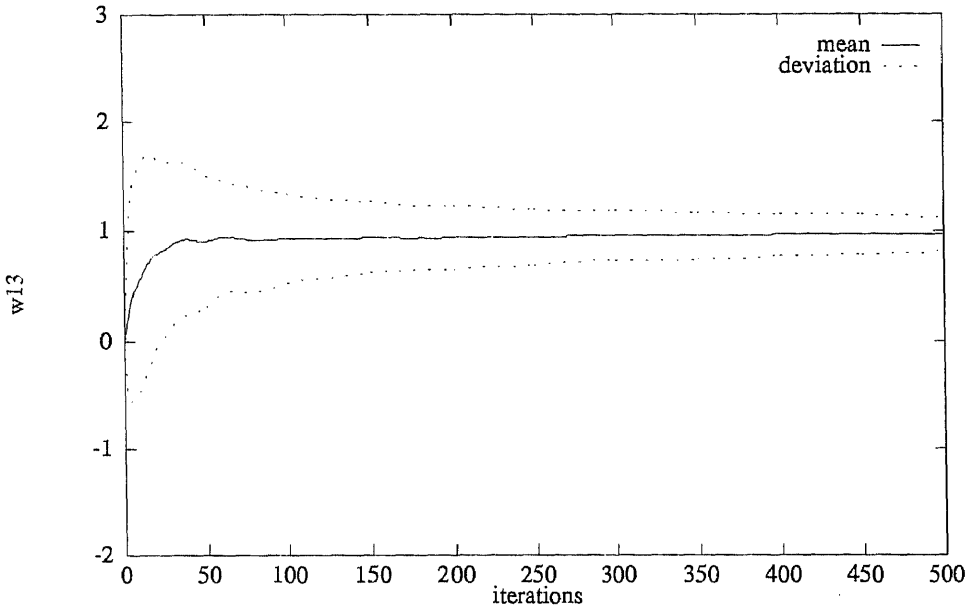


**Figure 4.5** The ensemble behavior of the weight $w_{13}$ in convergence with $\mu = 0.2$

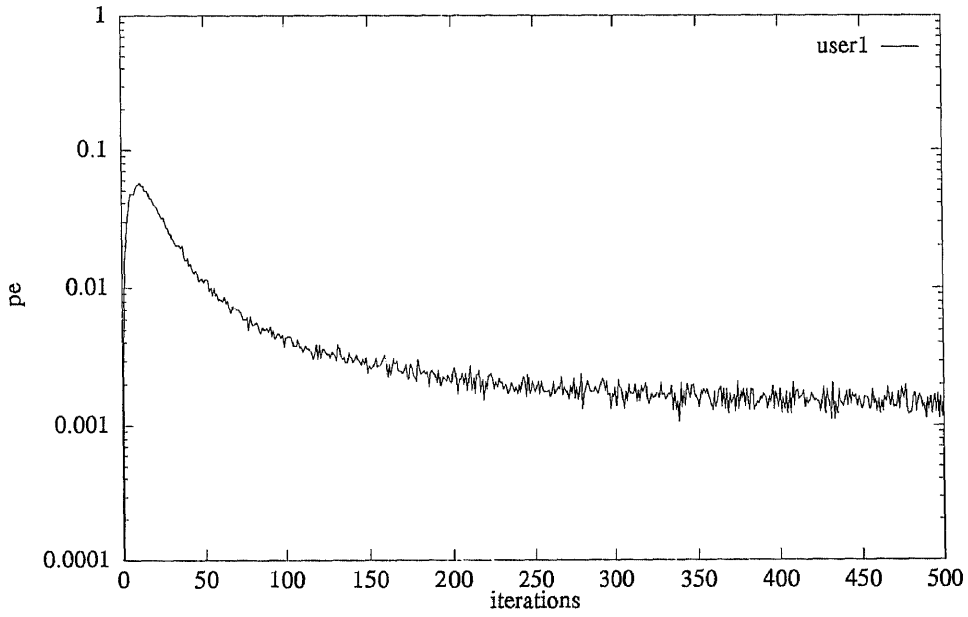


**Figure 4.6** The convergence of $Pe_1$ *with* $\mu = 0.2$ *and* $K = 3$

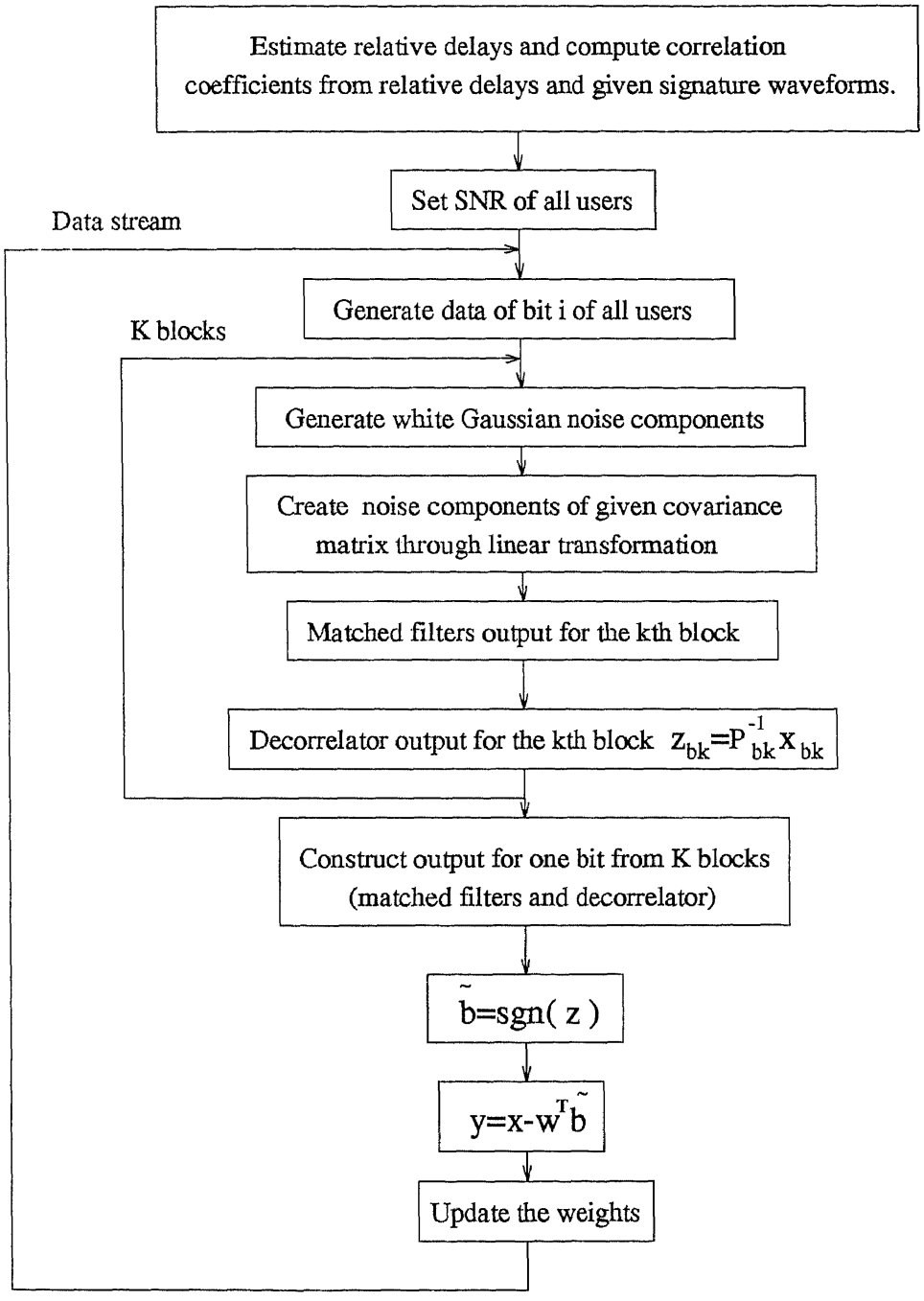


**Figure 4.7** Simulation flow chart

# CHAPTER 5

# ERROR PERFORMANCE AT THE OUTPUT

## 5.1 Evaluation of the Output Error Probability

The output error probability is evaluated as follows:

$$\begin{aligned} P_{e_1} &= Pr\{y_1 > 0 | b_1 = -1\} Pr\{b_1 = -1\} \\ &+ Pr\{y_1 < 0 | b_1 = 1\} Pr\{b_1 = 1\}. \end{aligned}$$

Since

$$Pr\{y_1 > 0 | b_1 = -1\} = Pr\{y_1 < 0 | b_1 = 1\},$$

and

$$Pr\{b_1 = -1\} = Pr\{b_1 = 1\} = \frac{1}{2},$$

$$\begin{aligned} P_{e_1} &= Pr\{y_1 > 0 | b_1 = -1\} \\ &= Pr\{-\sqrt{a_1} + \boldsymbol{\rho}_1^T \boldsymbol{A}_1 \boldsymbol{b}_1 - \boldsymbol{w}_1^T \tilde{\boldsymbol{b}}_1 + n_1 > 0\} \\ &= Pr\{n_1 > \sqrt{a_1} - \boldsymbol{\rho}_1^T \boldsymbol{A}_1 \boldsymbol{b}_1 + \boldsymbol{w}_1^T \tilde{\boldsymbol{b}}_1\} \\ &= \sum_{\boldsymbol{b}_1, \tilde{\boldsymbol{b}}_1} Pr\{n_1 > \sqrt{a_1} - \boldsymbol{\rho}_1^T \boldsymbol{A}_1 \boldsymbol{b}_1 + \boldsymbol{w}_1^T \tilde{\boldsymbol{b}}_1\} \\ &\quad \cdot Pr\{\tilde{\boldsymbol{b}}_1 | \boldsymbol{b}_1\} Pr\{\boldsymbol{b}_1\}. \end{aligned}$$

Since

$$Pr\{\boldsymbol{b}_1\} = 2^{-(2K-2)},$$

$$P_{e_1} = 2^{-(2K-2)} \sum_{\boldsymbol{b}_1, \tilde{\boldsymbol{b}}_1} [Pr\{n_1 > \sqrt{a_1} - \boldsymbol{\rho}_1^T \boldsymbol{A}_1 \boldsymbol{b}_1 + \boldsymbol{w}_1^T \tilde{\boldsymbol{b}}_1] Pr\{\tilde{\boldsymbol{b}}_1 | \boldsymbol{b}_1\}.$$

Finally,

$$P_{e_1} = 2^{-(2K-2)} \sum_{\boldsymbol{b}_1, \tilde{\boldsymbol{b}}_1} Q\left( \frac{\sqrt{a_1} - \boldsymbol{\rho}_1^T \boldsymbol{A}_1 \boldsymbol{b}_1 + \boldsymbol{w}_1^T \tilde{\boldsymbol{b}}_1}{\sqrt{N_0/2}} \right) Pr\{\tilde{\boldsymbol{b}}_1 | \boldsymbol{b}_1\}, \qquad (5.1)$$

where

$$Q(x) = \frac{1}{\sqrt{2\pi}} \int_x^\infty e^{-t^2/2} dt,$$

and $Pr\{\check{\boldsymbol{b}}_1 | \boldsymbol{b}_1\}$ is the integral of the $(2K-2)$-variate Gaussian density function:

$$Pr\{\check{\boldsymbol{b}}_1 | \boldsymbol{b}_1\} = \frac{1}{\sqrt{(2\pi)^{2K-2} |\boldsymbol{\Xi}_1|}}$$

$$\int_{\boldsymbol{\xi}_1^0}^{\infty} \cdots \int exp\left(-\frac{1}{2} \boldsymbol{\xi}_1^T \boldsymbol{\Xi}_1^{-1} \boldsymbol{\xi}_1\right) d\boldsymbol{\xi}_1, \tag{5.2}$$

while the elements of $\boldsymbol{\xi}_1^0$ are determined by $\tilde{b}_k(i)\xi_k(i) = -\sqrt{a_k} b_k(i)$ and $\tilde{b}_k(i-1)\xi_k(i-1) = -\sqrt{a_k} b_k(i-1)$, $\qquad k = 2, \ldots, K$.

The evaluation of Eq. (5.1) for the two-user case will be shown in Appendix C.

## 5.2 Numerical Results

In all the numerical examples below, the signal-to-noise ratio for user k is defined as $SNR_k = a_k/N_0$. ALl the numerical results are derived by evaluating Eq.(5.1).

Figure 5.1 shows, the probability of error of user 1 versus $SNR_1$ for two asynchronous users. The relative energy $e_1$ is defined as $e_1 = \int_{\tau_2}^{T} s_1^2(t) dt$. The case labeled (1) in the figure corresponds to a relatively weak level of interference. It describes a rather unfavorable scenario for this multistage detector due to tentative decisions which are not too reliable. This results in the performance of the detector at higher values of $SNR_1$ to be somewhat inferior to the decorrelator, whose performance is insensitive to the level of interference. However, the multistage detector outperforms the conventional detector. When the interference is stronger (case (2)), due to the reliable tentative decisions, the multistage detector by far outperforms the other two.

Figure 5.2 shows the probability of error versus the relative interference energy for the fixed $SNR_1$. The multistage detector clearly outperforms the decorrelator, and achieves the single-user bound for the relative interference level above 5 dB.

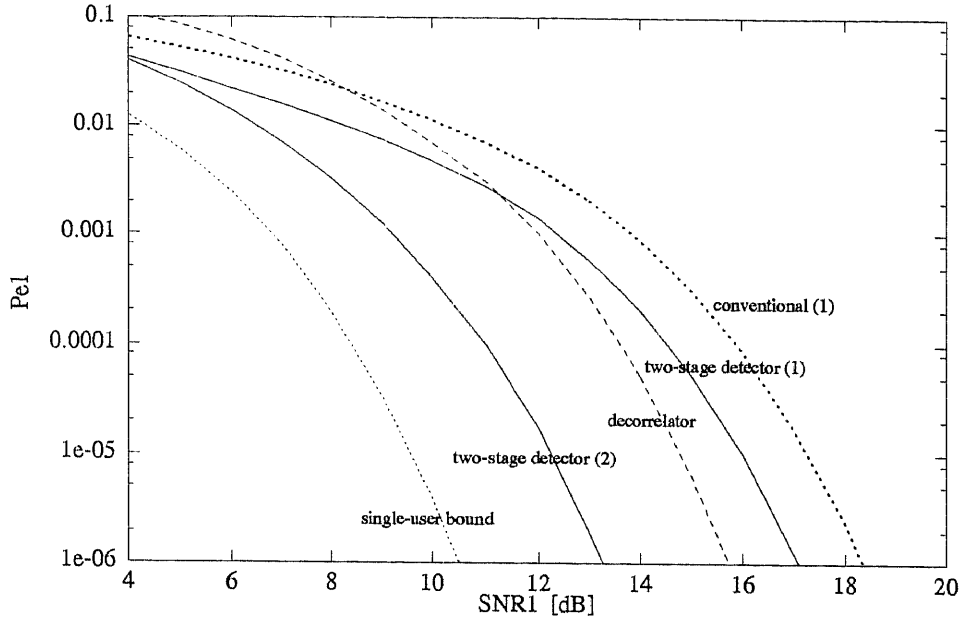


**Figure 5.1**: Error probability of user 1 for $K = 2$, $\rho_{12} = 0.2$, $\rho_{21} = 0.6$, $e_1 = 0.4$ (1) $a_2/a_1 = 0.6$ (2) $a_1/a_2 = 0.6$

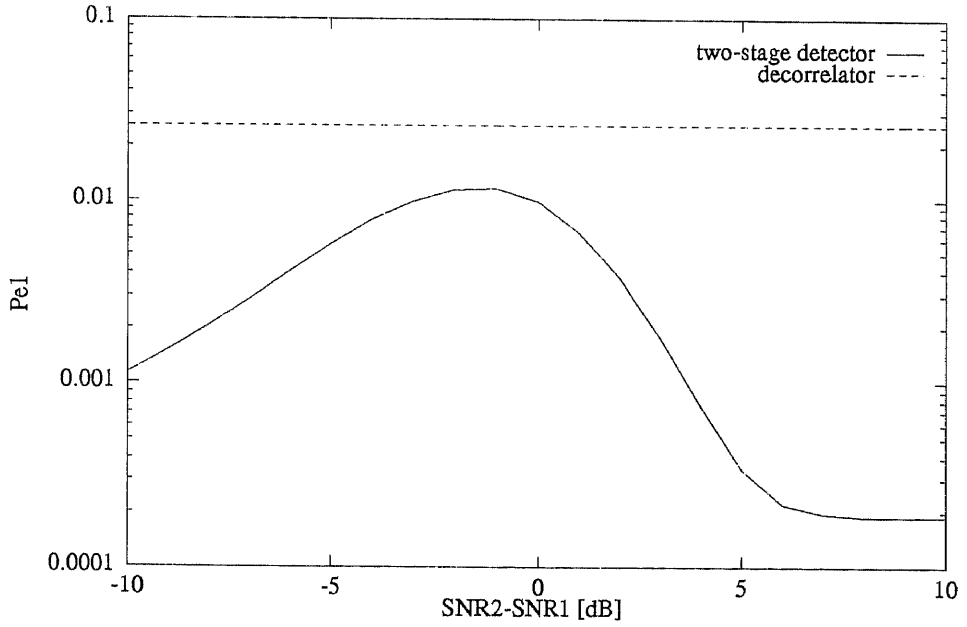


**Figure 5.2**: Error probability of user 1 for $K = 2$, $SNR_1 = 8\ dB$, $\rho_{12} = 0.2$, $\rho_{21} = 0.6$, $e_1 = 0.4$

The two signature sequences used in Figure 5.3 are gold sequences of length 7, $s_1(t)$ and $s_2(t)$ of Figure 5.6. Figure 5.3 shows the probability of error for user 1 when the energy of user 1 and the energy of the interferer are the same. The worst case and the average error performance over the values of the relative delay $\tau_2$ are shown. In this scenario the multistage detector outperforms both the conventional and the decorrelating detector, and its average performance, due to the good crosscorrelation properties of the two signature sequences used, is very close to the single user-bound. Note that the energy of user 1 and the energy of the interferer are the same means perfect power control, a condition that is the best for the conventional detector and very unfavorable to the multistage detector. Even so, the multistage detector outperforms the conventional detector by far.

Gold sequences of length 7, $s_1(t)$, $s_2(t)$ and $s_3(t)$ of Figure 5.6, are used as the signature sequences in the next two examples. Figure 5.4 shows the distribution of the error probability of user 1 over the relative delays $\tau_2$ and $\tau_3$, with the $SNR's$ of all three users equal to 12 dB. It is obvious that the error probability is very sensitive to the timing of all users. Nevertheless, it still has overall performance much better than those of the decorrelating detector and the conventional detector. The probability of error of the multistage detector, averaged over all delay pairs is $7 \times 10^{-5}$. (The corresponding values for the decorrelator and the conventional receiver are $9.4 \times 10^{-4}$ and $1.2 \times 10^{-2}$, respectively.)

Figure 5.5 shows the probability of error versus the relative interference energies for $SNR_1$ fixed to 8 dB, and $\tau_2 = T/7$, $\tau_3 = 5T/7$. Again, the multistage detector performs better than the decorrelator and approaches the single user bound as the interferers' energies increase.

The gold sequences used as the signature sequences in all the above numerical examples are included in Figure 5.6 for convenience.

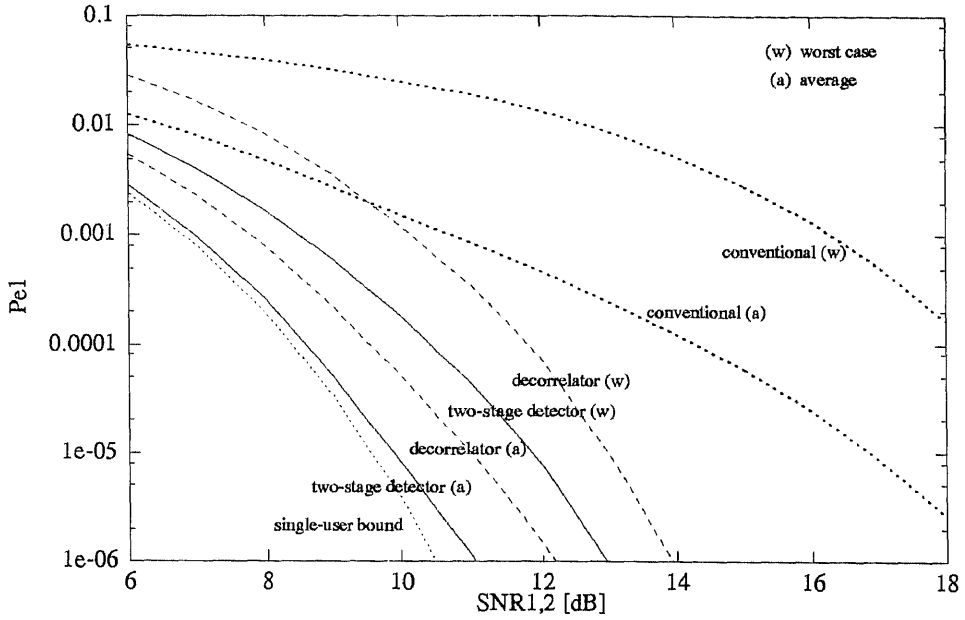


**Figure 5.3** Error probability of user 1 for $K = 2$

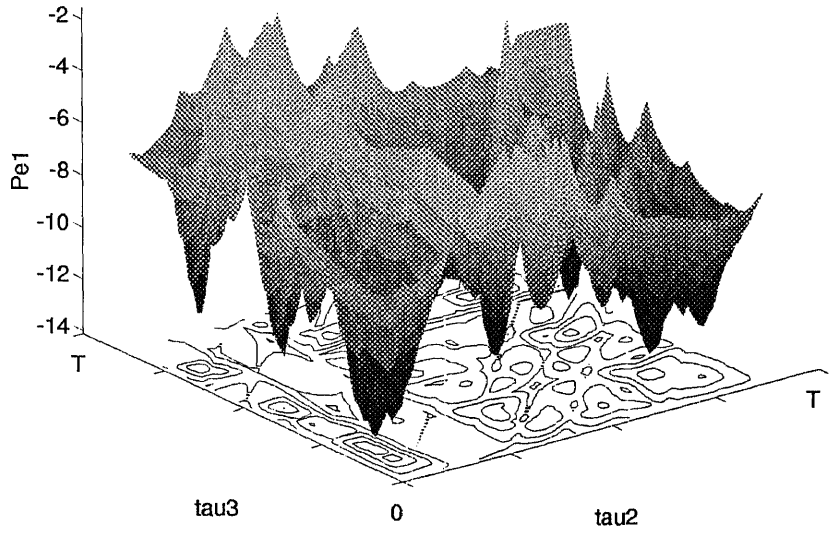


**Figure 5.4** Error probability of user 1 for K=3, $SNR_i = 12\ dB,\ i = 1, 2, 3$

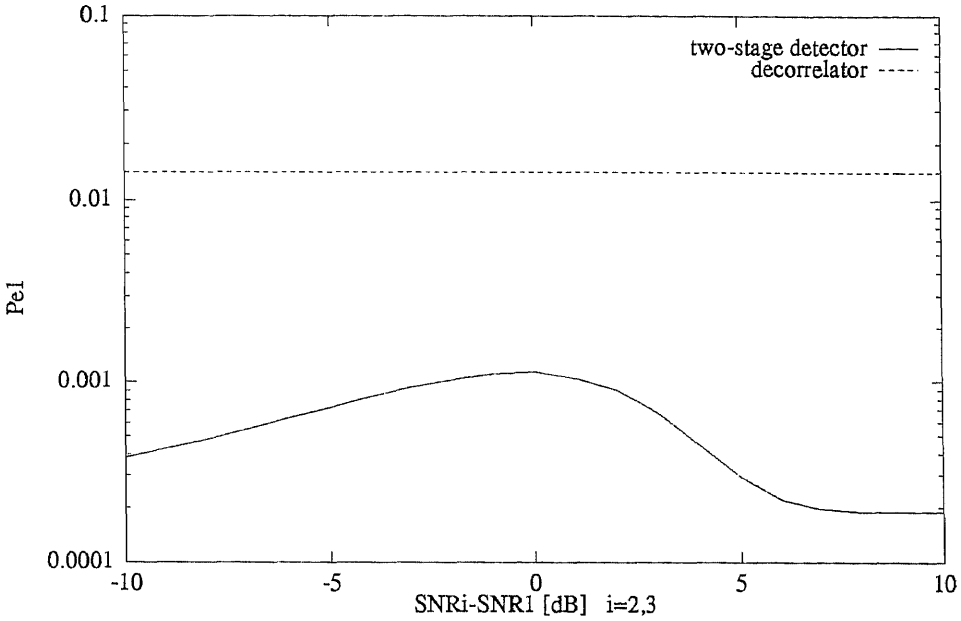


**Figure 5.5** Error probability of user 1 for K=3, $SNR_1 = 8\ dB$

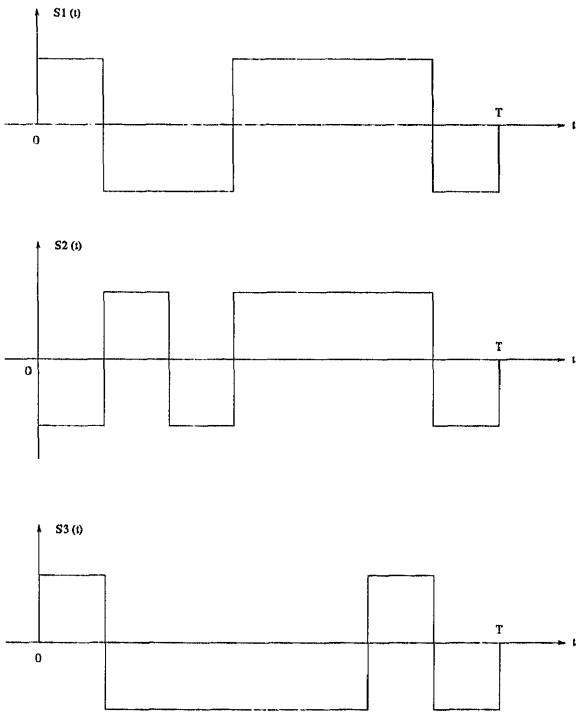


**Figure 5.6** Gold sequences

# CHAPTER 6

## CONCLUSION

An adaptive CDMA receiver scheme in an asynchronous channel has been proposed in this thesis. It has linear complexity with the number of users and is near-far resistant. But its most important feature is that it is adaptive and requires no knowledge of the received amplitude of any user. This is essential to mobile communications, since it can dynamically adapt to changes in users' power and eliminates the need for high-precision power control and user power estimation.

The drawback of the scheme is that its performance is sensitive to the relative delays of the users and it suffers degradation when its first stage has an singularity problem.

# APPENDIX A

## Decorrelator (two-user case)

To illustrate the general case in Chapter 3, the derivations of the fomula for the two-user case are presented here in detail. Let us consider each symbol interval separately, the bit $i$ of user 1, which occupies the interval $[0,T]$(assuming, without loss of generality, $\tau_2 > \tau_1 = 0$), overlaps with bit $i-1$ of user 2 over the interval $[0,\tau_2]$ and with bit $i$ of user 2 over the interval $[\tau_2,T]$. We can view the situation in the interval $[0,\tau_2]$ as a two-user synchronous channel with unit-energy signature waveforms $\bar{s}_{1L}(t) = \frac{s_{1L}(t)}{\sqrt{e_L}}, \bar{s}_{2L}(t) = \frac{s_{2L}(t)}{\sqrt{e_L}}$,
where $s_{1L}(t) = \begin{cases} s_1(t), & 0 < t < \tau_2 \\ 0, & \tau_2 < t < T \end{cases}$ $s_{2L}(t) = \begin{cases} s_2(t+T-\tau_2), & 0 < t < \tau_2 \\ 0, & \tau_2 < t < T \end{cases}$
and

$$e_L = \int_0^{\tau_2} s_1(t)^2 dt = \int_0^{\tau_2} s_2(t+T-\tau_2)^2 dt = \int_0^T s_{1L}(t)^2 dt = \int_0^T s_{2L}(t)^2 dt$$

is the partial energy of the signals over the left overlapping interval. We now follow the steps taken in the synchronous case.

The two-user white Guassian asynchronous multiple-access channel for the interval $[0,\tau_2]$ is:

$$r(t) = \sqrt{e_L}[\sqrt{a_1}b_1(i)\bar{s}_{1L}(t) + \sqrt{a_2}b_2(i-1)\bar{s}_{2L}(t)] + n(t) \tag{A.1}$$

The sampled outputs of the bank of matched filters that matched to $\bar{s}_{1L}(t)$ and $\bar{s}_{2L}(t)$ correspondingly can be expressed as:

$$\begin{bmatrix} x_{1L}(i) \\ x_{2L}(i) \end{bmatrix} = \sqrt{e_L}\mathcal{P}_L \boldsymbol{A} \begin{bmatrix} b_{1L}(i) \\ b_{2L}(i-1) \end{bmatrix} + \boldsymbol{n}_L(i) \tag{A.2}$$

where

$$\mathcal{P}_L = \begin{bmatrix} 1 & \frac{1}{e_L}\rho_{12L} \\ \frac{1}{e_L}\rho_{12L} & 1 \end{bmatrix} \quad and \quad \boldsymbol{A} = \begin{bmatrix} \sqrt{a_1} & 0 \\ 0 & \sqrt{a_2} \end{bmatrix}$$

and $\rho_{12L} = \int_0^T s_{1L}(t)s_{2L}(t)dt$ and $\boldsymbol{n}_L(i)$ is the filtered Gussian noise random vector with covariance $E\{\boldsymbol{n}_L\boldsymbol{n}_L^T\} = \frac{N_0}{2}\boldsymbol{\mathcal{P}}_L$.

The outputs of the decorrelator for the interval $[0, \tau_2]$ are given as:

$$\begin{bmatrix} z_{1L}(i) \\ z_{2L}(i) \end{bmatrix} = \boldsymbol{\mathcal{P}}_L^{-1} \begin{bmatrix} x_{1L}(i) \\ x_{2L}(i) \end{bmatrix} = \sqrt{e_L}\boldsymbol{A} \begin{bmatrix} b_1(i) \\ b_2(i-1) \end{bmatrix} + \boldsymbol{\xi}_L \tag{A.3}$$

where $\boldsymbol{\xi}_L = \begin{bmatrix} \xi_{1L}(i) \\ \xi_{2L}(i) \end{bmatrix} = \boldsymbol{\mathcal{P}}_L^{-1}\boldsymbol{n}_L = \boldsymbol{\Gamma}_L\boldsymbol{n}_L$ and

$$\boldsymbol{\Gamma}_L = \boldsymbol{\mathcal{P}}_L^{-1} = \frac{1}{1-\rho_{12L}^2/e_L^2} \begin{bmatrix} 1 & \frac{1}{e_L}\rho_{12L} \\ \frac{1}{e_L}\rho_{12L} & 1 \end{bmatrix}$$

Since $E\{\boldsymbol{n}_L\boldsymbol{n}_L^T\} = \frac{N_0}{2}\boldsymbol{\mathcal{P}}_L$ and $\boldsymbol{\Gamma}_L = \boldsymbol{\mathcal{P}}_L^{-1}$,

$$E\{\boldsymbol{\xi}_L\boldsymbol{\xi}_L^T\} = E\{(\boldsymbol{\Gamma}_L\boldsymbol{n}_L)(\boldsymbol{\Gamma}_L\boldsymbol{n}_L)^T\} = \boldsymbol{\Gamma}_L E\{\boldsymbol{n}_L\boldsymbol{n}_L^T\}\boldsymbol{\Gamma}_L^T = \frac{N_0}{2}\boldsymbol{\Gamma}_L \tag{A.4}$$

therefore, $Var(\xi_{1L}) = \frac{N_0}{2}\Gamma_{L11}$, while $\Gamma_{L11}$ is the first diagonal element of the matrix $\boldsymbol{\Gamma}_L$ and $\Gamma_{L11} = \frac{1}{1-\rho_{12L}^2/e_L^2}$.

We can also view the situation in the interval $[\tau_2, T]$ as a two-user synchronous channel with unit-energy signature waveforms $\bar{s}_{1R}(t) = \frac{1}{\sqrt{e_R}}s_{1R}(t), \bar{s}_{2R}(t) = \frac{1}{\sqrt{e_R}}s_{2R}(t)$, where $s_{1R}(t) = \begin{cases} 0 & 0 < t < \tau_2 \\ s_1(t) & \tau_2 < t < T \end{cases}$ $s_{2R}(t) = \begin{cases} 0 & 0 < t < \tau_2 \\ s_2(t-\tau_2) & \tau_2 < t < T, \end{cases}$

and

$$e_R = \int_0^T s_{1R}(t)^2 dt = \int_0^T s_{2R}(t)^2 dt.$$

Define

$$\boldsymbol{\mathcal{P}}_R = \begin{bmatrix} 1 & \frac{1}{e_R}\rho_{12R} \\ \frac{1}{e_R}\rho_{12R} & 1 \end{bmatrix}$$

where $\rho_{12R} = \int_0^T s_{1R}(t)s_{2R}(t)dt$, and

$$\boldsymbol{\Gamma}_R = \boldsymbol{\mathcal{P}}_R^{-1} = \frac{1}{1-\rho_{12R}^2/e_R^2} \begin{bmatrix} 1 & \frac{1}{e_R}\rho_{12R} \\ \frac{1}{e_R}\rho_{12R} & 1 \end{bmatrix}.$$

Following the same steps above, we can get the outputs of the decorrelator for the interval $[\tau_2, T]$:

$$\begin{bmatrix} z_{1R}(i) \\ z_{2R}(i) \end{bmatrix} = \sqrt{e_R}\boldsymbol{A} \begin{bmatrix} b_1(i) \\ b_2(i) \end{bmatrix} + \boldsymbol{\xi}_R(i), \tag{A.5}$$

where $\boldsymbol{\xi}_R(i) = \begin{bmatrix} \xi_{1R}(i) \\ \xi_{2R}(i) \end{bmatrix}$ and $E\{\boldsymbol{\xi}_R \boldsymbol{\xi}_R^T\} = \frac{N_0}{2}\boldsymbol{\Gamma}_R$. Therefore $Var(\xi_{1R}) = \frac{N_0}{2}\Gamma_{R11}$, while $\Gamma_{R11}$ is the first diagonal element of the matrix $\boldsymbol{\Gamma}_R$ and $\Gamma_{R11} = \frac{1}{1-\rho_{12R}^2/e_R^2}$.

The decorrelator outputs for the i-th symbol interval are constructed as the weighted sum of those of the interval $[0, \tau_2]$ and $[\tau_2, T]$. Without loss of generality, attention is focused on user 1 only.

The decorrelator output for the i-th symbol interval of user 1 is:

$$z_1(i) = c_{1L} z_{1L}(i) + c_{1R} z_{1R}(i). \tag{A.6}$$

The weights are selected in such a way that the error probability at the outputs of the decorrelator are minimized. The optimum weights selected are:

$$c_{1L} = \frac{\sqrt{e_L}}{\Gamma_{L11}}\Gamma_{11} \quad c_{1R} = \frac{\sqrt{e_R}}{\Gamma_{R11}}\Gamma_{11} \tag{A.7}$$

where

$$\Gamma_{11} = \frac{1}{\frac{e_L}{\Gamma_{L11}} + \frac{e_R}{\Gamma_{R11}}} = \frac{1}{1 - \rho_{12L}^2/e_L - \rho_{12R}^2/e_R}$$

Substituting the optimum weights into Eq.(A.6), we have

$$\begin{aligned} z_1(i) &= \frac{\sqrt{e_L}}{\Gamma_{L11}}\Gamma_{11}\sqrt{e_L}\sqrt{a_1}b_1(i) + \frac{\sqrt{e_R}}{\Gamma_{R11}}\Gamma_{11}\sqrt{e_R}\sqrt{a_1}b_1(i) + \xi_1(i) \\ &= (\frac{e_L}{\Gamma_{L11}} + \frac{e_R}{\Gamma_{R11}})\Gamma_{11}\sqrt{a_1}b_1(i) + \xi_1(i) \\ &= \sqrt{a_1}b_1(i) + \xi_1(i) \end{aligned} \tag{A.8}$$

where

$$\xi_1(i) = \frac{\sqrt{e_L}}{\Gamma_{L11}}\Gamma_{11}\xi_{1L} + \frac{\sqrt{e_R}}{\Gamma_{R11}}\Gamma_{11}\xi_{1R}$$

and

$$Var(\xi_1) = \Gamma_{11}^2[\frac{e_L}{\Gamma_{L11}^2}Var(\xi_{1L}) + \frac{e_R}{\Gamma_{R11}^2}Var(\xi_{1R})] = \frac{N_0}{2}\Gamma_{11}^2[\frac{e_L}{\Gamma_{L11}} + \frac{e_R}{\Gamma_{R11}}] = \frac{N_0}{2}\Gamma_{11}. \tag{A.9}$$

The tentative decision at the output of the decorrelator for user 1 is $\tilde{b}_1(i) = \mathrm{sgn}(z_1(i))$.

The corresponding error probability is evaluated as:

$$\begin{aligned} Pr\{\tilde{b}_1(i) \text{ in error}\} &= Pr\{\tilde{b}_1(i) = 1 | b_1(i) = -1\} Pr\{b_1(i) = -1\} \\ &+ Pr\{\tilde{b}_1(i) = -1 | b_1(i) = 1\} Pr\{b_1(i) = 1\} \end{aligned}$$

Since the channel is a BSC channel,

$$Pr\{\tilde{b}_1(i) = 1 | b_1(i) = -1\} = Pr\{\tilde{b}_1(i) = -1 | b_1(i) = 1\}$$

and $$Pr\{b_1(i) = 1\} = Pr\{b_1(i) = -1\} = \tfrac{1}{2}$$

$$\begin{aligned} Pr\{\tilde{b}_1(i) \text{ in error}\} &= Pr\{\tilde{b}_1(i) = 1 | b_1(i) = -1\} \\ &= Pr\{z_1(i) > 0 | b_1(i) = -1\} \\ &= Pr\{-\sqrt{a_1} + \xi_1 > 0\} \\ &= Pr\{\xi_1 > \sqrt{a_1}\} \\ &= Q\left(\sqrt{\frac{a_1}{Var(\xi_1)}}\right) \\ &= Q\left(\sqrt{\frac{a_1}{\frac{N_0}{2}\Gamma_{11}}}\right). \end{aligned} \tag{A.10}$$

# APPENDIX B

## Weights (two-user case)

The sampled output of the matched filter for user 1 is:

$$x_1(i) = \sqrt{a_1}b_1(i) + \sqrt{a_2}\left[\rho_{21}b_2(i-1) + \rho_{12}b_2(i)\right] + n_1(i).$$

The normalized partial cross-correlations are:

$$\rho_{21} = \int_0^T s_1(t)s_2(t+T-\tau_2)dt \quad \text{and} \quad \rho_{12} = \int_0^T s_1(t)s_2(t-\tau_2)dt.$$

Also, $n_1(i) = \int_0^T n(t)s_1(t)dt$ is a zero-mean Gaussian random variable with variance $N_0/2$.

The multistage detector subtracts the weighted sum of the tentative estimates of the interference afflicted with user 1 from the matched filter output. The final decision is:

$$y_1(i) = x_1(i) - \boldsymbol{w}_1^T(i)\tilde{\boldsymbol{b}}_1(i) = x_1(i) - w_{21}\tilde{b}_2(i-1) - w_{12}\tilde{b}_2(i),$$

where $\boldsymbol{w}_1(i) = [w_{21}, w_{12}]^T$ are the corresponding weights, and $\tilde{\boldsymbol{b}}_1(i) = [\tilde{b}_2(i-1), \tilde{b}_2(i)]^T$ is the tentative decision vector affecting user 1.

### B.1 Weight Updating

Without loss of generality, we focus our attention on the weight $w_{21}$.

The output can be expressed as

$$\begin{aligned} y_1(i) &= x_1(i) - w_{21}\tilde{b}_2(i-1) - w_{12}\tilde{b}_2(i) \\ &= \sqrt{a_1}b_1(i) + \sqrt{a_2}[\rho_{21}b_2(i-1) + \rho_{12}b_2(i)] + n_1(i) - w_{21}\tilde{b}_2(i-1) - w_{12}\tilde{b}_2(i) \\ &= \sqrt{a_1}b_1(i) + [\sqrt{a_2}\rho_{21}b_2(i-1) - w_{21}\tilde{b}_2(i-1)] + [\sqrt{a_2}\rho_{12}b_2(i) - w_{12}\tilde{b}_2(i)] \\ &+ n_1(i). \end{aligned}$$

The output noise-plus-interference power can be obtained by subtracting the output signal power $a_1$ from the output power $E\{y_1^2(i)\}$. Thus, the output SNIR, defined as the ratio between the output signal power and the sum of the output noise and interference power, can be calculated from

$$SNIR = \frac{a_1}{E\{y_1^2(i)\} - a_1}. \tag{B.1}$$

It is obvious that by selecting weights such that the ouput power $E\{y_1^2(i)\}$ is minimized, we can achieve maximum output SNIR, which is a good measurement of the performance of the spread spectrum system.

So the steepest descent algorithm which minimizes the ouput power $E\{y_1^2(i)\}$ , and which therefore maximizes the output SNIR, is used to train the weights:

$$\begin{aligned} w_{21}(i+1) &= w_{21}(i) - \frac{\mu}{2}\frac{\partial}{\partial w_{21}(i)}E\{y_1^2(i)\} \\ &= w_{21}(i) + \mu E\{y_1(i)\tilde{b}_2(i-1)\} \end{aligned}$$

Substitute $y_1(i) = x_1(i) - w_{21}\tilde{b}_2(i-1) - w_{12}\tilde{b}_2(i)$ into it, and we get

$$\begin{aligned} w_{21}(i+1) &= w_{21}(i) + \mu E\{[x_1(i) - w_{21}\tilde{b}_2(i-1) - w_{12}\tilde{b}_2(i)]\tilde{b}_2(i-1)\} \\ &= w_{21}(i) + \mu E\{x_1(i)\tilde{b}_2(i-1)\} - \mu w_{21}E\{\tilde{b}_2^2(i-1)\} \\ &- \mu w_{12}E\{\tilde{b}_2(i)\tilde{b}_2(i-1)\} \end{aligned}$$

Since $\tilde{b}_2(i-1)$ and $\tilde{b}_2(i)$ are decisions made on two non-overlapping intervals, they are uncorrelated, i.e. $E\{\tilde{b}_2(i)\tilde{b}_2(i-1)\} = 0$. And it is obvious that $\tilde{b}_2^2(i-1) \equiv 1$, thus $E\{\tilde{b}_2^2(i-1)\} = 1$. So we get:

$$w_{21}(i+1) = (1-\mu)w_{21}(i) + \mu E\{x_1(i)\tilde{b}_2(i-1)\} \tag{B.2}$$

## B.2 Steady State Values of the Weight

As has been proved in Chapter 4, the above iterative search will converge if $0 < \mu < 1$ and the weight $w_{21}$ will reach the steady state value $w_{21}^0$, which satisfies

$$w_{21}^0 = (1-\mu)w_{21}^0 + \mu E\{x_1(i)\tilde{b}_2(i-1)\}$$

From it, we can easily get the steady state value of the weight $w_{21}$, which is:

$$w_{21}^0 = E\{x_1(i)\tilde{b}_2(i-1)\}$$

We can also verify that the above $w_{21}^0$ satisfies the equation $\frac{\partial}{\partial w_{21}^0} E\{y_1^2(i)\} = 0$, which means when the weights reach the steady values, the output power will be minimized, and the system in the steady state will have the optimum SNIR.

The above expectation can be further evaluated by substituting $x_1(i) = \sqrt{a_1}b_1(i) + \sqrt{a_2}[\rho_{21}b_2(i-1) + \rho_{12}b_2(i)] + n_1(i)$ into it, and we have

$$\begin{aligned} w_{21} &= E\{[x_1(i)\tilde{b}_2(i-1)\} \\ &= E\{[\sqrt{a_1}b_1(i) + \sqrt{a_2}[\rho_{21}b_2(i-1) + \rho_{12}b_2(i)] + n_1(i)]\tilde{b}_2(i-1)\} \\ &= \sqrt{a_1}E\{b_1(i)\tilde{b}_2(i-1)\} + \sqrt{a_2}\rho_{21}E\{b_2(i-1)\tilde{b}_2(i-1)\} \\ &+ \sqrt{a_2}\rho_{12}b_2(i)\tilde{b}_2(i-1)\} + E\{n_1(i)\tilde{b}_2(i-1)\}. \end{aligned}$$

Since we are using the one-shot, decorrelated, tentative decision in the first stage, which is interference-free, it is obvious that $E\{b_1(i)\tilde{b}_2(i-1)\} = 0$; and from the good properties of the decorrelator proved before $E\{n_1(i)\xi_2(i-1)\} = 0$, we will have $E\{n_1(i)\tilde{b}_2(i-1)\} = 0$, since $\tilde{b}_2(i-1)$ is interference-free and only related to $b_2(i-1)$ and $\xi_2(i-1)$, and the former is obviously independent of $n_1(i)$. Finally, we will also have $E\{b_2(i)\tilde{b}_2(i-1)\} = 0$, which is simply because the intervals they are related to are not overlapping.

Now the above expression will be greatly simplified, and we have

$$w_{21}^0 = \sqrt{a_2}\rho_{21}E\{b_2(i-1)\tilde{b}_2(i-1)\}. \tag{B.3}$$

With the knowledge of the error probability at the decorrelator output, we can easily compute the $w_{21}^0$ in terms of error functions.

$$\begin{aligned} E\{b_2(i-1)\tilde{b}_2(i-1)\} &= Pr\{b_2(i-1)\tilde{b}_2(i-1) = 1\} \cdot 1 \\ &+ Pr\{b_2(i-1)\tilde{b}_2(i-1) = -1\} \cdot (-1) \end{aligned}$$

$$
\begin{aligned}
&= Pr\{b_2(i-1)\tilde{b}_2(i-1)=1\} \\
&- Pr\{b_2(i-1)\tilde{b}_2(i-1)=-1\} \\
&= [1-Pr\{b_2(i-1)\tilde{b}_2(i-1)=1\}] \\
&- Pr\{b_2(i-1)\tilde{b}_2(i-1)=-1\} \\
&= 1-2Pr\{b_2(i-1)\tilde{b}_2(i-1)=-1\} \\
&= 1-2Pr\{\tilde{b}_2(i-1) \text{ in error}\} \\
&= 1-2Q\left(\sqrt{\frac{a_2}{\frac{N_0}{2}\Gamma_{22}}}\right) \\
&= erf\left(\sqrt{\frac{a_2}{\frac{N_0}{2}\Gamma_{22}}}\right).
\end{aligned}
$$

So the final result is:

$$
w_{21}^0 = \sqrt{a_2}\rho_{21} erf\left(\sqrt{\frac{a_2}{\frac{N_0}{2}\Gamma_{22}}}\right), \tag{B.4}
$$

where

$$
\Gamma_{22} = \Gamma_{11} = \frac{1}{1-\frac{\rho_{12L}^2}{e_L}-\frac{\rho_{12R}^2}{e_R}}
$$

In the two-user case, $\rho_{12L} = \rho_{21}$, $\rho_{12R} = \rho_{12}$ and $e_1 = e_R$, $e_L + e_R = 1$.

## APPENDIX C

### Error Probability at the Output (two-user case)

From Eq.(5.1), note that $\hat{b}_2(i-1)$ and $\tilde{b}_2(i)$ are independent, we evaluate the error probability at the output of user 1 for the two-user case as follows:

$$P_{e_1} = \frac{1}{4} Pr\{\tilde{b}_2(i-1)|b_2(i-1)\} Pr\{\tilde{b}_2(i)|b_2(i)\}$$
$$\sum_{\substack{b_2(i-1),\, b_2(i) \\ \tilde{b}_2(i-1),\, \tilde{b}_2(i)}} Q\left(\frac{\sqrt{a_1} - \rho_{21}\sqrt{a_2}b_2(i-1) - \rho_{12}\sqrt{a_2}b_2(i) + w_{21}\tilde{b}_2(i-1) + w_{12}\tilde{b}_2(i)}{\sqrt{N_0/2}}\right)$$

From Eq.(A.10),

$$Pr\{\tilde{b}_2(i) = \pm 1 | b_2(i) = \mp 1\} = Q\left(\sqrt{\frac{a_2}{\frac{N_0}{2}\Gamma_{22}}}\right),$$

and

$$\begin{aligned} Pr\{\tilde{b}_2(i) = \pm 1 | b_2(i) = \pm 1\} &= 1 - Pr\{\tilde{b}_2(i) = \pm 1 | b_2(i) = \mp 1\} \\ &= 1 - Q\left(\sqrt{\frac{a_2}{\frac{N_0}{2}\Gamma_{22}}}\right). \end{aligned}$$

Since the system is stationary, the same is true for bit $i-1$.

With this knowledge, we can evaluate the error probability at the output of user 1 as

$$\begin{aligned} P_{e_1} &= \left[ Q\left(\frac{\sqrt{a_1} - \rho_{21}\sqrt{a_2} - \rho_{12}\sqrt{a_2} + w_{21} + w_{12}}{\sqrt{N_0/2}}\right)\right. \\ &+ Q\left(\frac{\sqrt{a_1} - \rho_{21}\sqrt{a_2} + \rho_{12}\sqrt{a_2} + w_{21} - w_{12}}{\sqrt{N_0/2}}\right) \\ &+ Q\left(\frac{\sqrt{a_1} + \rho_{21}\sqrt{a_2} + \rho_{12}\sqrt{a_2} - w_{21} - w_{12}}{\sqrt{N_0/2}}\right) \\ &+ \left. Q\left(\frac{\sqrt{a_1} + \rho_{21}\sqrt{a_2} - \rho_{12}\sqrt{a_2} - w_{21} + w_{12}}{\sqrt{N_0/2}}\right)\right] \end{aligned}$$

$$
\begin{aligned}
&\cdot \quad \frac{1}{4}\left[1-Q\left(\sqrt{\frac{a_2}{\frac{N_0}{2}\Gamma_{22}}}\right)\right]^2 \\
&+ \quad \left[Q\left(\frac{\sqrt{a_1}+\rho_{21}\sqrt{a_2}+\rho_{12}\sqrt{a_2}+w_{21}+w_{12}}{\sqrt{N_0/2}}\right)\right. \\
&+ \quad Q\left(\frac{\sqrt{a_1}-\rho_{21}\sqrt{a_2}+\rho_{12}\sqrt{a_2}-w_{21}+w_{12}}{\sqrt{N_0/2}}\right) \\
&+ \quad Q\left(\frac{\sqrt{a_1}+\rho_{21}\sqrt{a_2}-\rho_{12}\sqrt{a_2}+w_{21}-w_{12}}{\sqrt{N_0/2}}\right) \\
&+ \quad \left.Q\left(\frac{\sqrt{a_1}-\rho_{21}\sqrt{a_2}-\rho_{12}\sqrt{a_2}-w_{21}-w_{12}}{\sqrt{N_0/2}}\right)\right] \\
&\cdot \quad \frac{1}{4}Q\left(\sqrt{\frac{a_2}{\frac{N_0}{2}\Gamma_{22}}}\right)^2 \\
&+ \quad \left[Q\left(\frac{\sqrt{a_1}-\rho_{21}\sqrt{a_2}-\rho_{12}\sqrt{a_2}+w_{21}-w_{12}}{\sqrt{N_0/2}}\right)\right. \\
&+ \quad Q\left(\frac{\sqrt{a_1}-\rho_{21}\sqrt{a_2}+\rho_{12}\sqrt{a_2}+w_{21}+w_{12}}{\sqrt{N_0/2}}\right) \\
&+ \quad Q\left(\frac{\sqrt{a_1}+\rho_{21}\sqrt{a_2}+\rho_{12}\sqrt{a_2}-w_{21}+w_{12}}{\sqrt{N_0/2}}\right) \\
&+ \quad Q\left(\frac{\sqrt{a_1}+\rho_{21}\sqrt{a_2}-\rho_{12}\sqrt{a_2}-w_{21}-w_{12}}{\sqrt{N_0/2}}\right) \\
&+ \quad Q\left(\frac{\sqrt{a_1}-\rho_{21}\sqrt{a_2}-\rho_{12}\sqrt{a_2}-w_{21}+w_{12}}{\sqrt{N_0/2}}\right) \\
&+ \quad Q\left(\frac{\sqrt{a_1}-\rho_{21}\sqrt{a_2}+\rho_{12}\sqrt{a_2}-w_{21}-w_{12}}{\sqrt{N_0/2}}\right) \\
&+ \quad Q\left(\frac{\sqrt{a_1}+\rho_{21}\sqrt{a_2}+\rho_{12}\sqrt{a_2}+w_{21}-w_{12}}{\sqrt{N_0/2}}\right) \\
&+ \quad \left.Q\left(\frac{\sqrt{a_1}+\rho_{21}\sqrt{a_2}-\rho_{12}\sqrt{a_2}+w_{21}+w_{12}}{\sqrt{N_0/2}}\right)\right] \\
&\cdot \quad \frac{1}{4}Q\left(\sqrt{\frac{a_2}{\frac{N_0}{2}\Gamma_{22}}}\right)\left[1-Q\left(\sqrt{\frac{a_2}{\frac{N_0}{2}\Gamma_{22}}}\right)\right]. \qquad \text{(C.1)}
\end{aligned}
$$

## APPENDIX D

### Expectations

Without loss of generality, we assume $i = 0$, although the conclusions below will be true for any symbol interval of user 1.

The elements on the main diagonal of $E\left\{\tilde{\boldsymbol{b}}_1(0)\tilde{\boldsymbol{b}}_1^T(0)\right\}$ are equal to unity, while the off-diagonal ones are:

$$\begin{aligned} & E\left\{\tilde{b}_k(i)\tilde{b}_l(j)\right\} \\ = \; & E\left\{\operatorname{sgn}\left(\sqrt{a_k}b_k(i)+\xi_k(i)\right)\operatorname{sgn}\left(\sqrt{a_l}b_l(j)+\xi_l(j)\right)\right\} \\ = \; & \frac{1}{2}\sum_{b_k(i),b_l(j)}\left[Pr\{\xi_k(i) < \sqrt{a_k}b_k(i)\,,\,\xi_l(j) < \sqrt{a_l}b_l(j)\right\} \\ & - Pr\{\xi_k(i) < \sqrt{a_k}b_k(i)\;,\;\xi_l(j) > \sqrt{a_l}b_l(j)\}] \\ & i,j = -1,0 \qquad k,l = 2,\ldots,K \quad k \neq l \end{aligned}$$

Each probability term in the above summation defines four integrals. Therefore:

$$E\{\tilde{b}_k(i)\tilde{b}_l(j)\} = \frac{(-1)^m}{2}\sum_{m=1}^{8}\int\int_{D_m} f_{\xi_k\xi_l}d\xi_k d\xi_l \tag{D.1}$$

where $f_{\xi_k\xi_l}$ denotes the bivariate Gaussian density function of random variables $\xi_k(i)$ and $\xi_l(j)$, and $D_m$ is an appropriate rectangular region of integration.

The diagonal elements of $E\left\{\boldsymbol{b}_1(0)\tilde{\boldsymbol{b}}_1^T(0)\right\}$ are:

$$\begin{aligned} E\{b_k(i)\tilde{b}_k(i)\} \;&=\; 1 - 2Q\left(\sqrt{\frac{a_k}{\sigma_{\xi_k}^2}}\right) \\ & \qquad k = 2,\ldots,K \quad i = -1,0 \end{aligned} \tag{D.2}$$

with

$$Q(x) = \frac{1}{\sqrt{2\pi}}\int_x^\infty e^{-t^2/2}dt$$

# APPENDIX E

## System Structure

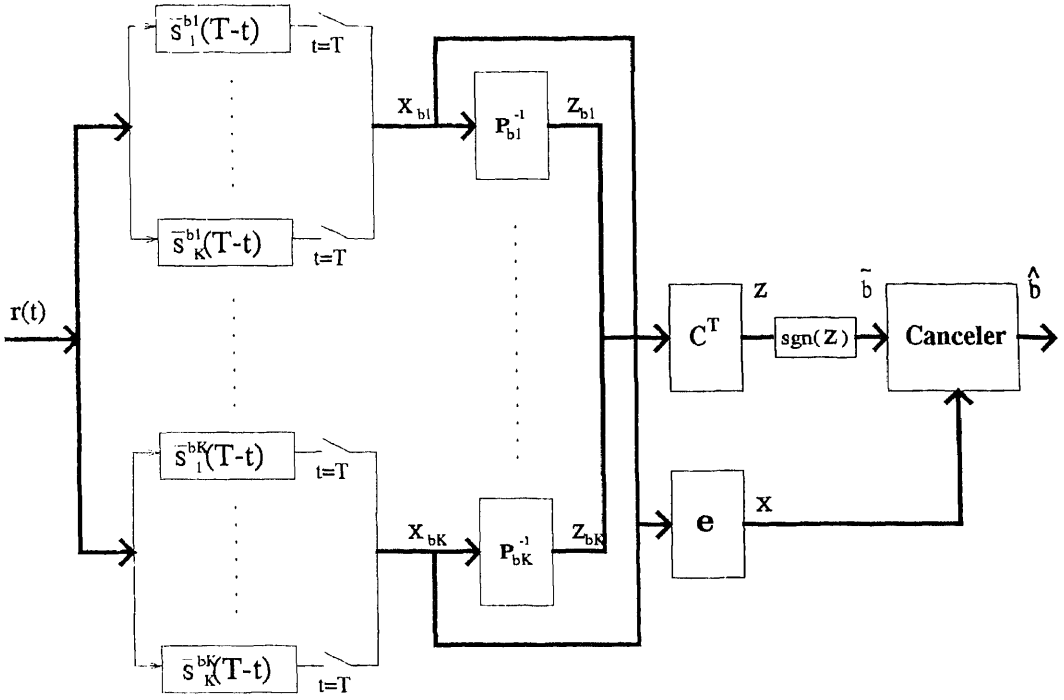


**Figure E.1** System structure

Note that the waveforms of the matched filters are dependent on the relative delays. So analog filters can not be used here since the relative delays are not known in advance. DSP processors that can be programmable should be used to implement the matched filters.

In the above diagram, $\boldsymbol{x}_b = [\boldsymbol{x}_{b1}, \boldsymbol{x}_{b2}, \ldots, \boldsymbol{x}_{bK}]$, $\boldsymbol{e} = [\sqrt{e_{b1}}, \sqrt{e_{b2}}, \ldots, \sqrt{e_{bK}}]^T$ and $\boldsymbol{x} = \boldsymbol{x}_b\boldsymbol{e}$. The decorrelator output are $z_k = \boldsymbol{c}_k^T \boldsymbol{z}_{kb}$, where $\boldsymbol{z}_{kb} = [z_{kb1}, z_{kb2}, \ldots, z_{kbK}]$, $k = 1, 2, \ldots, K$. To construct the matched filter and the decorrelator output for a user other than user 1, the outputs of some blocks should be shifted to make the outputs of all blocks correspond to the same symbol interval of that user.

The number of matched filters used is K per user. In this sense, the complexity of the receiver is linear with the number of users. The order of the cross-correlation matrices is K. It is obvious that the inverse operations of K matrices of order K need much less computation power than the inverse operation of a single matrix of order $2K-2$. And one of the impressive advantages of the receiver is that the parallel processing can be used.

## REFERENCES


1. S. Verdu, "Minimum probability of error for asynchronous Gaussian multiple-access channels," *IEEE Trans. on Information Theory*, vol. 32, no.1, pp. 85–96, January 1986.

2. R. Lupas and S. Verdu, "Linear multiuser detectors for synchronous code-division multiple-access channels," *IEEE Trans. on Information Theory*, vol. 35, no. 1, pp. 123–136, January 1989.

3. R. Lupas and S. Verdu, "Near-far resistance of multiuser detectors in asynchronous channels," *IEEE Trans. on Communications*, vol. 38, no. 4, pp. 496-508, April 1990.

4. M. K. Varanasi and B. Aazhang, "Multistage detection in asynchronous code-division multiple-access communications," *IEEE Trans. on Communications*, vol. 38, no. 4, pp. 509–519, April 1990.

5. M. K. Varanasi and B. Aazhang, "Near-optimum detection in synchronous code-division multiple-access communications," *IEEE Trans. on Communications*, vol. 39, no. 5, pp. 725–736, May 1991.

6. A. Duel-Hallen, "Decision-feedback multiuser detector for synchronous code-division multiple access channel," *IEEE Trans. on Communications*, vol. 41, no. 2, pp. 285–290, February 1993.

7. Z. Xie, C. K. Rushforth, and R. T. Short, "Multi-user signal detection using sequential decoding," *IEEE Trans. on Communications*, pp. 578–583, May 1990.

8. Z. Xie, R. T. Short, and C. K. Rushforth, "A family of suboptimum detectors for coherent multi-user communications," *IEEE Journal on Selected Areas in Communications*, pp. 683–690, May 1990.

9. S. Verdu, "Adaptive multiuser detection," *Proceedings of the 3rd IEEE International Symposium on Spread Spectrum Techniques and Applications*, Oulu, Finland, July 1994.

10. P.B. Rapajic and B.S. Vucetic, "Adaptive receiver structures for asynchronous CDMA systems," *IEEE Journal on Selected Areas in Communications*, vol. 12, no. 4, pp. 685-697, May 1994.

11. M. Honig, U. Madhow, and S. Verdu, "Blind adaptive interference supression for near-far resistant CDMA," *1994 IEEE Globecom*, December 1994. accepted. Also patent pending.

12. B.P. Paris, "Asymptotic properties of self-adaptive maximum-likelihood sequence estimation," *Proc. 1993 Conf. Information Sciences and Systems*, pp. 161–166, John Hopkins University, Baltimore, MD., 1993.

13. Z. Siveski, Y. Bar-Ness, and D.W. Chen, "Error performance of synchronous multiuser code division multiple access detector with multidimensional adaptive canceler," *European Transactions on Telecommunications and Related Technologies*, accepted for publication.

14. B. Zhu, N. Ansari, Z. Siveski, and Y. Bar-Ness, "Convergence and stability analysis of a synchronous adaptive CDMA receiver," submitted to *IEEE Trans. on Communications.*

15. Z. Siveski, L. Zhong, and Y. Bar-Ness, "An adaptive multiuser CDMA detector for asynchronous AWGN channels," *Proceedings of the 5th IEEE International Symposium on Personal, Indoor and Mobile Radio Communications*, The Hague, The Netherlands, September 1994.

16. M. Marcus and H. Minc, *A Survey of Matrix Theory and Matrix Inequality*, Allyn and Bacon, Inc., Boston, MA., 1964.